Reduction of cortical parvalbumin-expressing GABAergic interneurons in a rodent hyperoxia model of preterm birth brain injury with deficits in social behavior and cognition.

Scheuer T., Auf dem Brinke E., Grosser S., Wolf S.A., Mattei D., Sharkovska Y., Barthel P.C., Endesfelder S., Friedrich V., Bührer C., Vida I., Schmitz T.

Development
2021 OCT 14 ; 148(20): dev198390
doi: 10.1242/dev.198390
Publisher: The Company of Biologists Ltd

© 2021. Published by The Company of Biologists Ltd | Development (2021) 148, dev198390. doi:10.1242/dev.198390

RESEARCH ARTICLE

Reduction of cortical parvalbumin-expressing GABAergic interneurons in a rodent hyperoxia model of preterm birth brain injury with deficits in social behavior and cognition

Till Scheuer[1,*], Elena auf dem Brinke[1], Sabine Grosser[2], Susanne A. Wolf[3,4], Daniele Mattei[3,5], Yuliya Sharkovska[1,6,7], Paula C. Barthel[1,6], Stefanie Endesfelder[1], Vivien Friedrich[1,7], Christoph Bührer[1], Imre Vida[2] and Thomas Schmitz[1]

ABSTRACT

The inhibitory GABAergic system in the brain is involved in the etiology of various psychiatric problems, including autism spectrum disorders (ASD), attention deficit hyperactivity disorder (ADHD) and others. These disorders are influenced not only by genetic but also by environmental factors, such as preterm birth, although the underlying mechanisms are not known. In a translational hyperoxia model, exposing mice pups at P5 to 80% oxygen for 48 h to mimic a steep rise of oxygen exposure caused by preterm birth from *in utero* into room air, we documented a persistent reduction of cortical mature parvalbumin-expressing interneurons until adulthood. Developmental delay of cortical myelin was observed, together with decreased expression of oligodendroglial glial cell-derived neurotrophic factor (GDNF), a factor involved in interneuronal development. Electrophysiological and morphological properties of remaining interneurons were unaffected. Behavioral deficits were observed for social interaction, learning and attention. These results demonstrate that neonatal oxidative stress can lead to decreased interneuron density and to psychiatric symptoms. The obtained cortical myelin deficit and decreased oligodendroglial GDNF expression indicate that an impaired oligodendroglial-interneuronal interplay contributes to interneuronal damage.

KEY WORDS: Preterm birth, Cortical interneurons, Oxidative stress, Oligodendroglial GDNF, ADHD, ASD

INTRODUCTION

Preterm birth is one of the major pediatric public health problems of our time with 1-2% of all live births being preterm. Although in earlier studies, brain tissue injury in preterm infants was often found to be due to tissue destruction and necrosis, leading to cystic brain lesions, nowadays a more subtle form of brain injury is much more characteristic (de Kieviet et al., 2009; Larroque et al., 2008; Penn et al., 2016). This includes deficits in cognition and motor development, but is also reflected in a high incidence of psychiatric problems, such as attention deficit hyperactivity disorder (ADHD) and autism spectrum disorder (ASD) (Johnson and Marlow, 2011; Limperopoulos et al., 2008; Lindström et al., 2011). A cell population that has increasingly been linked to various psychiatric diseases is the group of inhibitory GABAergic (γ-aminobutyric acid) interneurons (Edden et al., 2012; Hashemi et al., 2017; Nakazawa et al., 2012; Northoff and Sibille, 2014). GABAergic interneurons represent up to 25-30% of neurons in the cortex (Wonders and Anderson, 2006), and they play a central role in orchestrating neuronal activity. Different sub-populations of cortical interneurons are generated from distinct regions of the ganglionic eminence: parvalbumin- (PVALB) or somatostatin (SST)-positive interneurons are generated from the medial ganglionic eminence (MGE), while reelin- (RELN) or vasoactive intestinal peptide (VIP)-expressing interneurons are derived from the caudal ganglionic eminence (CGE) (Hu et al., 2017; Rudy et al., 2011). In humans, generation and migration of GABAergic interneuron peaks between gestational weeks 16 and 35 (Achim et al., 2014; Arshad et al., 2016). A decrease of GABAergic interneurons could be linked to preterm birth and to white matter pathologies in preterm infants (Lacaille et al., 2019; Panda et al., 2018; Stolp et al., 2019). Even though brain pathologies in preterm infants are often attributed to perinatal infection/inflammation, hypocapnia and hyperoxia, the underlying mechanisms leading to behavioral deficits and also to psychiatric diseases are poorly understood (Dammann and Leviton, 2004; Leviton et al., 2010; Penn et al., 2016; Volpe, 2009). Results from clinical studies suggest a link between higher oxygen saturation limits for the more earlier preterm infants on intensive care units and worse neurological outcome later on (Collins et al., 2001; Leviton et al., 2010). There are two major mechanisms through which high oxygen levels may interfere with the development of immature neural cells: by direct dysregulation of cellular pathways and, more nonspecifically, by oxidative stress. The tissue injury caused by oxidative stress has been shown to be induced by exposure to hyperoxia (Endesfelder et al., 2017; Felderhoff-Mueser et al., 2004; Schmitz et al., 2014) and is a characteristic finding in injured brain tissue after preterm birth (Haynes et al., 2009). Oxidative stress may impair neuronal development (Scheuer et al., 2018), increase apoptosis (Endesfelder et al., 2017) and induce autophagy (Bendix et al., 2012; Wyrsch et al., 2012). Besides these global toxic effects, oxygen is also more specifically a fundamental regulator of cell function and gene expression (Zhang et al., 2011). In neural progenitor and stem cells, lower oxygen tensions induce an increase of proliferation activity while higher oxygen levels lead to diminished proliferation (Rodrigues et al., 2010).

[1]Department of Neonatology, Charité – Universitätsmedizin Berlin, Berlin 13353, Germany. [2]Institute for Integrative Neuroanatomy, NeuroCure Cluster of Excellence, Charité – Universitätsmedizin Berlin, Berlin 10117, Germany. [3]Cellular Neurocience, Max-Delbrueck-Center for Molecular Medicine in the Helmholtz Association, Berlin 13125, Germany. [4]Department of Experimental Ophthalmology, Charité – Universitätsmedizin Berlin, Berlin 13353, Germany. [5]Institute of Pharmacology and Toxicology, University of Zurich-Vetsuisse, Zurich CH-8057, Switzerland. [6]Institute for Cell and Neurobiology, Center for Anatomy, Charité – Universitätsmedizin Berlin, Berlin 10117, Germany. [7]Berlin Institute of Health (BIH), Berlin 10178, Germany.

*Author for correspondence (till.scheuer@charite.de)

T.S., 0000-0002-9465-7200

Handling Editor: Paola Arlotta
Received 11 November 2020; Accepted 17 September 2021

Development (2021) 148, dev198390. doi:10.1242/dev.198390

Directly after birth, the arterial oxygen tension increases in preterm infants from 25 mmHg up to 60-80 mmHg, even without extra supply of oxygen (Castillo et al., 2008), hence reflecting a three- to fourfold increase in comparison to the prenatal, i.e. fetal, situation. This happens at a time when the oxidative stress defense system of the fetus, and also of the preterm baby, is still immature and has very low activity (Ikonomidou and Kaindl, 2011). To mimic the increase of oxygen disposability, we use a well-established hyperoxia model (Felderhoff-Mueser et al., 2004; Schmitz et al., 2012). Mice pups at postnatal day 5 (P5) were exposed to 80% oxygen for 48 h until age P7, which has previously been demonstrated to induce a three- to fourfold increase of oxygen levels and to delay white matter development in newborn mice (Schmitz et al., 2011). In this study, we are using this model in order to investigate the impact of oxygen and oxidative stress on GABAergic interneuron development and on psychiatric symptoms until young adult ages.

RESULTS

Decreased cortical expression of GABAergic interneuron markers after exposure to hyperoxia

Parvalbumin (PVALB), somatostatin (SST), vasoactive intestinal peptide (VIP) and reelin (RELN) expression can be used to distinguish the vast majority of cortical GABAergic interneurons (Hu et al., 2017). Precursors of PVALB$^+$ and SST$^+$ interneurons express the transcription factor LHX6 (Alifragis et al., 2004). To analyze the impact of perinatal 48 h exposure to hyperoxia from P5 to P7 on cortical interneuron development, we analyzed the RNA expression of *Lhx6*, *Sst*, *Reln* and *Vip* in mice cortices immediately after hyperoxia at P7, and also during recovery in room air at P9, P11, P14, P30 and P60. Western blot analysis was performed to identify the effect of long-term changes in cortical expression on protein level.

PVALB, the most prominent marker of GABAergic interneurons, starts to be expressed at around P12-P14 (de Lecea et al., 1995; Miyamae et al., 2017; Rudy et al., 2011) and was therefore analyzed at juvenile and adult ages P14, P30 and P60. RNA expression of *Pvalb* was significantly lower at P14 and P30 in animals with perinatal exposure to hyperoxia when compared with controls. At P60 there was a high tendency (P=0.07) of decreased *Pvalb* RNA expression (Fig. 1B). In the western blot analysis, PVALB protein expression was significantly reduced in cortical samples of hyperoxia exposed animals at all time points (P14, P30 and P60) (Fig. 1C,D).

Gene expression of *Lhx6*, as a marker proceeding PVALB$^+$ and SST$^+$ in immature interneurons, was lower at P9, P11 and P14, but levels were similar to controls at older ages (Fig. 1A). Gene expression of the markers for the other interneuron subunits *Sst*, *Reln* and *Vip* was lower at P9 and/or P11 and then similar to controls at older ages (Fig. 2A-C). At P14 and P30, western blot analysis

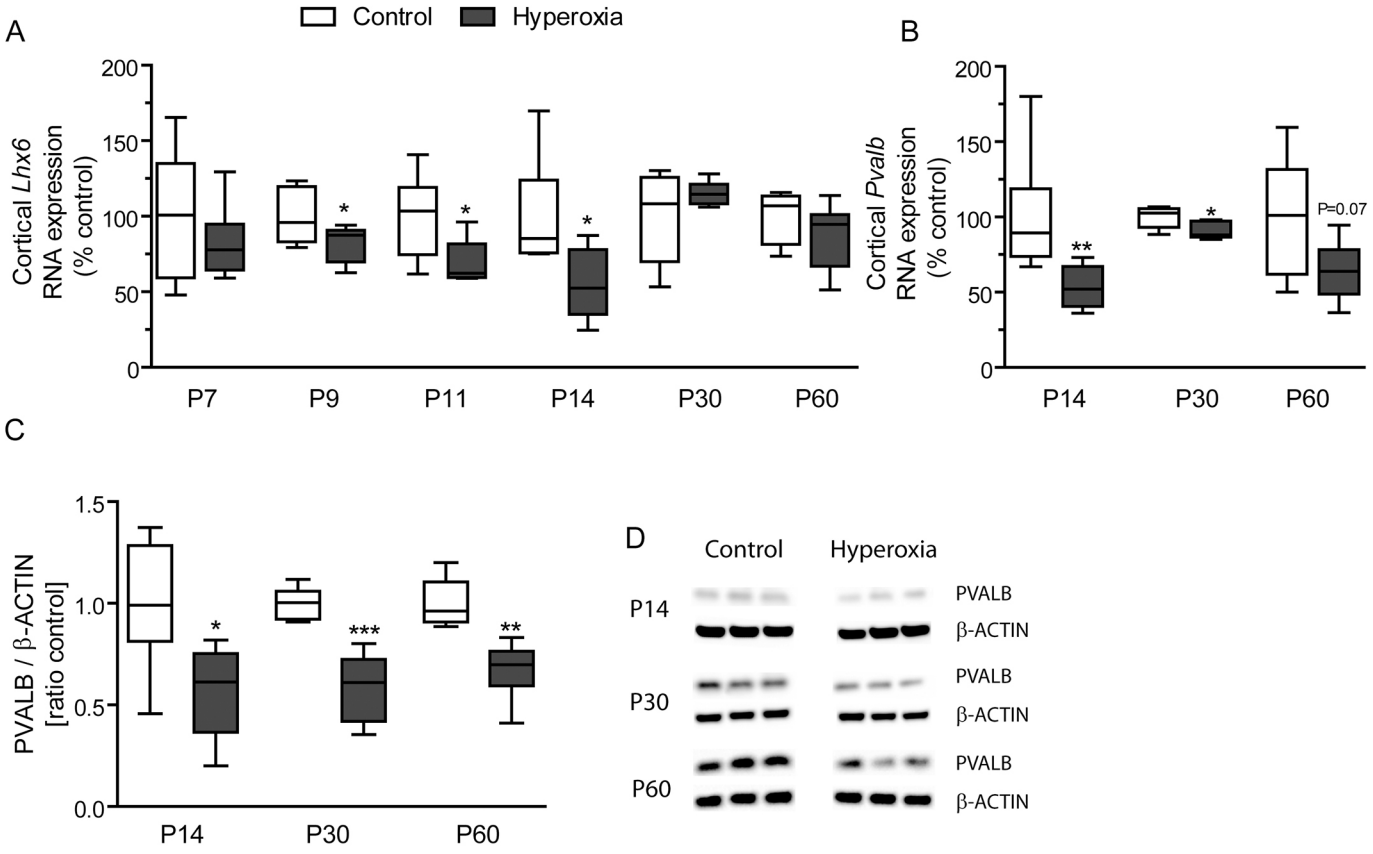

Fig. 1. Decreased cortical expression of interneuron subtype markers LHX6 and PVALB. (A,B) Real-time PCR analysis of the markers of GABAergic interneurons: LIM/homeobox protein 6 (*Lhx6*) and parvalbumin (*Pvalb*) at P7, P9, P11, P14, P30 and P60. (A) As a marker for immature SST$^+$ and immature PVALB$^+$ interneurons being derived from the medial ganglionic eminence, expression of *Lhx6* was reduced in cortical samples from animals exposed to hyperoxia at P9 (80%±5%), P11 (70%±6%) and P14 (55%±9.5%), while it returns to control level at P30 and P60. (B) Expression of the marker *Pvalb*, representing the major subtype of cortical GABAergic interneurons, starts at later time points during maturation. RNA expression analysis of *Pvalb* at P14, P30 and P60 reveals a significant reduction in hyperoxia animals at P14 (53%±5.5%) and P30 (90%±2%), while at P60, there was a tendency (P=0.07) for reduced *Pvalb* expression (64%±8%) [for qPCR: n=8 (P7), 7 (P9), 6 (P11-P60), t-test, Mann–Whitney U-test *P<0.05]. (C,D) Western blot analysis reveals decreased cortical PVALB expression at the ages P14 (0.57±0.1), P30 (0.58±0.07) and P60 (0.67±0.06) (for western blot: n=6; t-test: *P<0.05; **P<0.01, ***P<0.001). White bar, control; black bar, hyperoxia. The line in the center of the box plot indicates the median. Whiskers indicate the minimum and maximum.

Development (2021) 148, dev198390. doi:10.1242/dev.198390

revealed long-term recovery of cortical SST, RELN and VIP expression in mice that experienced hyperoxia (Fig. 2D-F).

Hyperoxia diminished the number of cortical PVALB-expressing interneurons

PVALB$^+$ interneurons are the main subgroup of GABAergic interneurons, representing 40% of all cortical interneurons in rodents (Rudy et al., 2011). Preterm birth is a risk factor for impaired PVALB$^+$ interneuron development (Panda et al., 2018) and oxidative challenges can alter PVALB$^+$ interneuron numbers in the cortex (Cabungcal et al., 2013). To verify the observed decrease of cortical parvalbumin expression on the cellular level, we performed immunohistochemical staining at P14, P30 and P60 for PVALB (Fig. 3A). During this developmental period, the number of PVALB$^+$ interneurons in the cortex increased dynamically in both groups (Fig. 3B). However, in the hyperoxia animals, cell density of cortical mature PVALB-expressing interneurons was significantly reduced in comparison with control litters at all three time points (Fig. 3B). Hence, these results show a persistent decrease in PVALB-expressing cortical interneurons caused by neonatal hyperoxia. In addition, immunohistochemical staining for SST and serotonin receptor 3A (HTR3A) indicated no decrease in the density of SST$^+$, RELN$^+$ and VIP$^+$ cortical interneurons at P14 and P30 (Fig. 4A-D). HTR3A was used as a marker for all GABAergic interneurons that express VIP and RELN (Rudy et al., 2011) (Fig. 4C,D).

Oxidative stress exposure did not alter apoptosis and autophagy

Oxidative stress represents a potentially toxic stimulus for neuronal cells that can also inhibit or damage PVALB$^+$ interneurons and result in behavioral disorders (Cabungcal et al., 2013; Jiang et al., 2013; Sorce et al., 2012). Immature neuronal cells have been shown to be vulnerable to oxidative stress (Ikonomidou and Kaindl, 2011). Hyperoxia can induce apoptosis and autophagy in the immature rodent brain (Bendix et al., 2012; Endesfelder et al., 2014). As oxidative stress can lead to lipid peroxidation (Yoshida et al., 2013), we evaluated levels of oxidative stress induced by 48 h hyperoxia

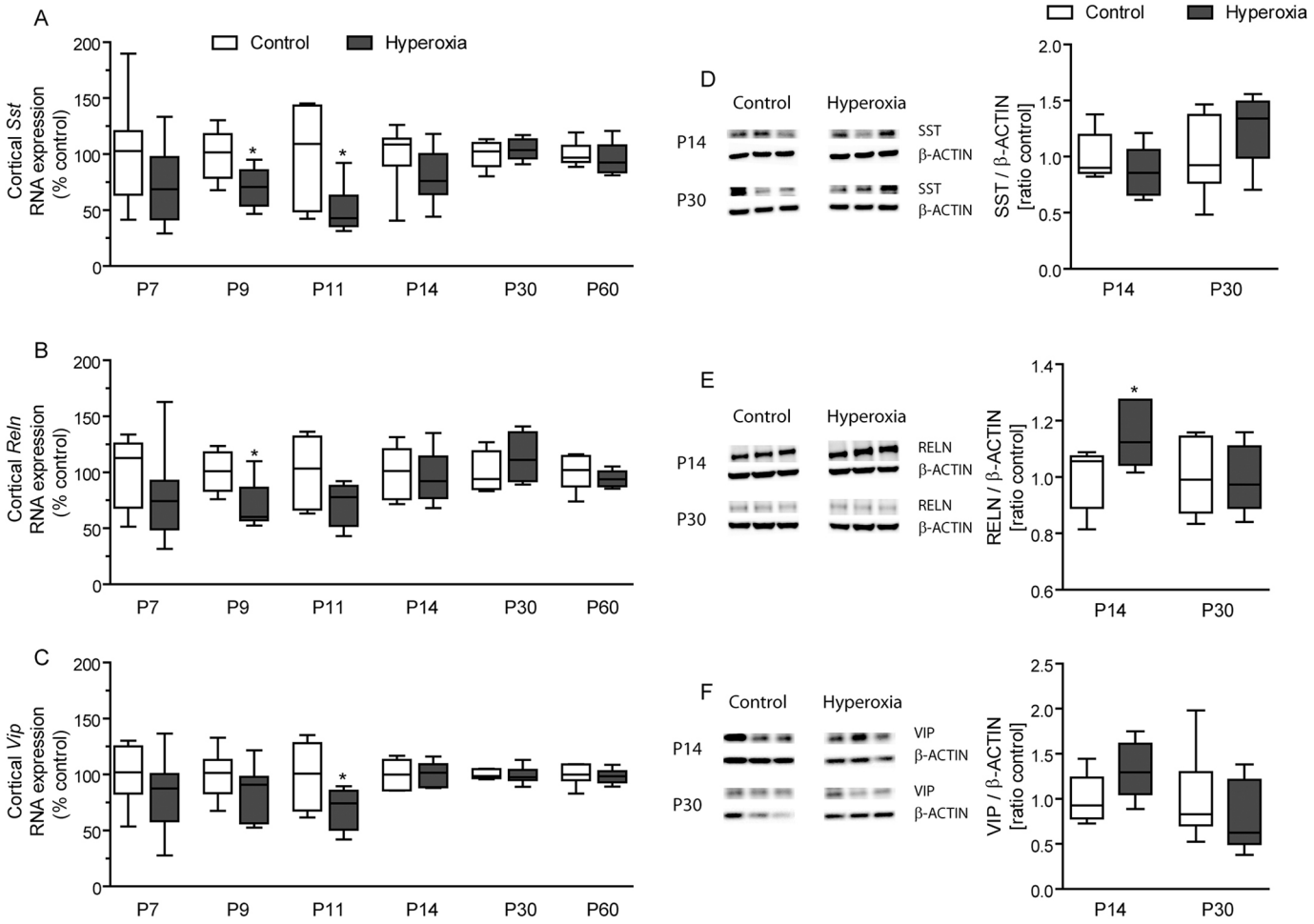

Fig. 2. Cortical expression of interneuron subtype markers SST, RELN and VIP. (A-C) Real-time PCR analysis of the markers of GABAergic interneurons: somatostatin (*Sst*), reelin (*Reln*) and vasoactive intestinal peptide (*Vip*) at P7, P9, P11, P14, P30 and P60. (A) *Sst* was reduced in cortices of hyperoxia-exposed animals at P9 (70%±6.5%) and P11 (50%±9%). At P14, *Sst* expression returns to levels of control litters. (B) RELN$^+$ and VIP$^+$ interneurons represent subtypes derived from the caudal ganglionic eminence. RNA expression of *Reln* was reduced at P11 (70±7%). (C) Cortical expression of *Vip* was reduced at P11 (70%±7.5%) and returned to control levels at P14 [for qPCR: n=8 (P7), 7 (P9), 6 (P11-P60); t-test, Mann–Whitney U-test: *P<0.05; **P<0.01]. (D-F) Western blot analysis reveals long-term recovery of cortical protein expression at P14 and P30. Cortical RELN expression was slightly increased (1.14±0.04) in animals exposed to hyperoxia at P14 (for western blot: n=6; t-test: *P<0.05). White bar, control; black bar, hyperoxia. The line in the center of the box plot indicates the median. Whiskers indicate the minimum and maximum.

Development (2021) 148, dev198390. doi:10.1242/dev.198390

in neonatal mouse brains by TBARS ELISA assay (Fig. 5D). As a result, we detected a more than twofold increase of lipid peroxidation in the hyperoxic mouse brain at the age P7. Hyperoxia-induced lipid peroxidation was reflected by increased expression of the glutamate-cysteine ligase catalytic subunit (*Gclc*) and superoxide dismutase 2 (*Sod2*) as a cellular response to oxidative stress in cortical samples at P7 (Fig. 5E,F).

To identify the impact of hyperoxia-induced oxidative stress on GABAergic interneuron apoptosis, we used transgenic GAD67-EGFP mice to analyze the number of cleaved caspase 3^+ (CASP3A) and $GAD67^+$ (GFP+) cells at P7, P9, P11 and P14 (Fig. 5A). Overall, the amount of cortical apoptosis and the number of apoptotic interneurons was very low. Hyperoxia exposure did not increase the numbers of $GAD67^+CASP3A^+$ interneurons at any of the analyzed time points (Fig. 5B). Moreover, qPCR analysis of *Casp3* expression in cortical samples did not reveal changes after hyperoxia (Fig. 5C). For analysis of autophagy activity, western blot analyses for LC3 and p62 were performed using cortical protein samples (Fig. 6A,B), and

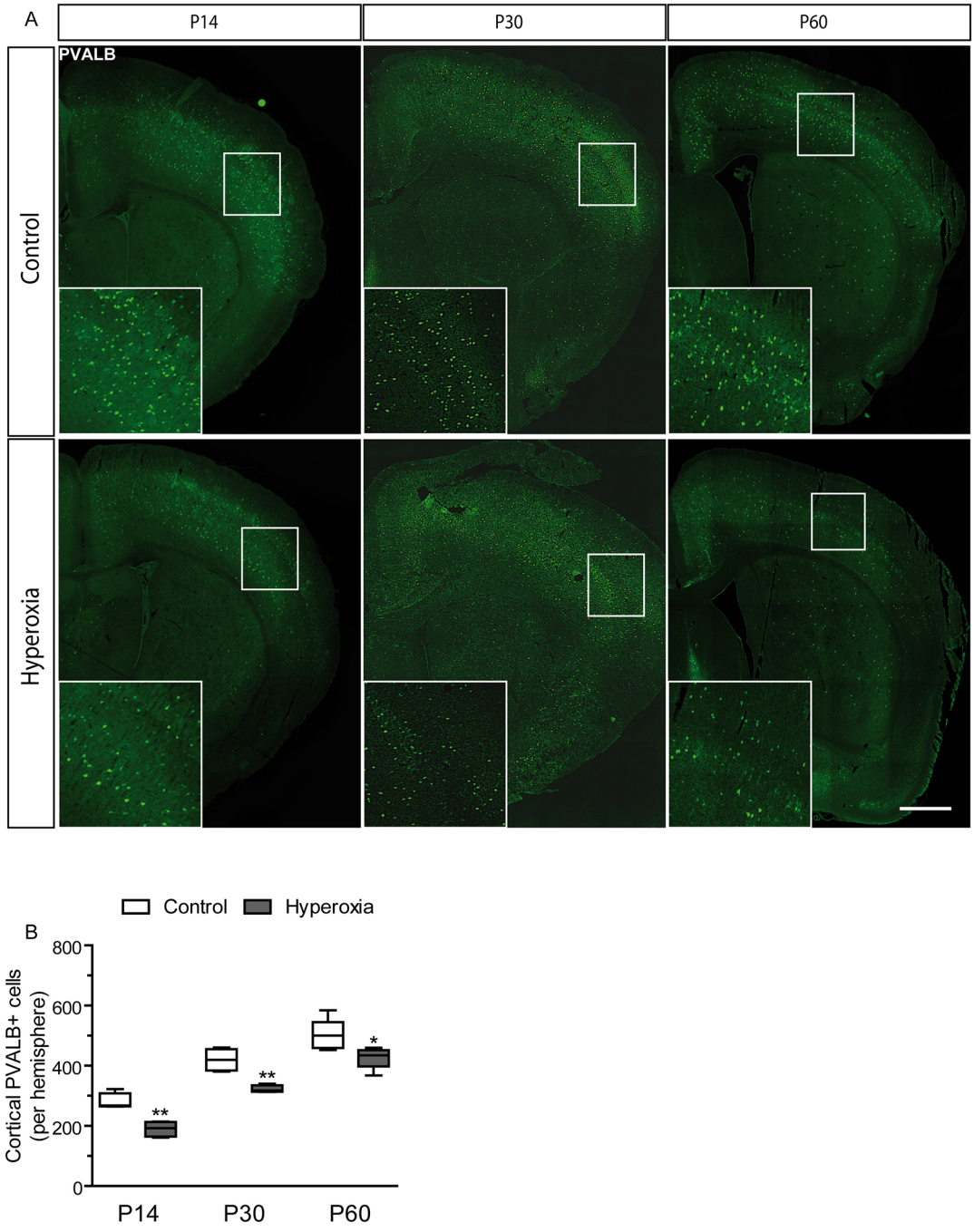

Fig. 3. Numbers of cortical $PVALB^+$ GABAergic interneurons. (A) $PVALB^+$ interneurons represent the main subgroup of GABAergic interneurons with 40% of all GABAergic interneurons being $PVALB^+$. Immunohistochemical staining for PVALB of 10 µm coronal brain sections obtained from mice after 48 h of neonatal hyperoxia (P5-P7) and controls at P14, P30 and P60. Insets show the areas outlined at higher magnification. (B) The number of cortical PVALB-expressing interneurons was largely reduced by neonatal hyperoxia at all ages analyzed, specifically at P14 (control=280±14 versus hyperoxia=190±13), P30 (control=420±19 versus hyperoxia=322±6) and P60 (control 502±23 versus hyperoxia=426±16) [n=4 (P14, P30) n=5 (P60); t-test, Mann–Whitney U-test: *P<0.05; **P<0.01]. Scale bar: 500 µm. White bar, control; black bar, hyperoxia. The line in the center of the box plot indicates the median. Whiskers indicate the minimum and maximum.

Development (2021) 148, dev198390. doi:10.1242/dev.198390

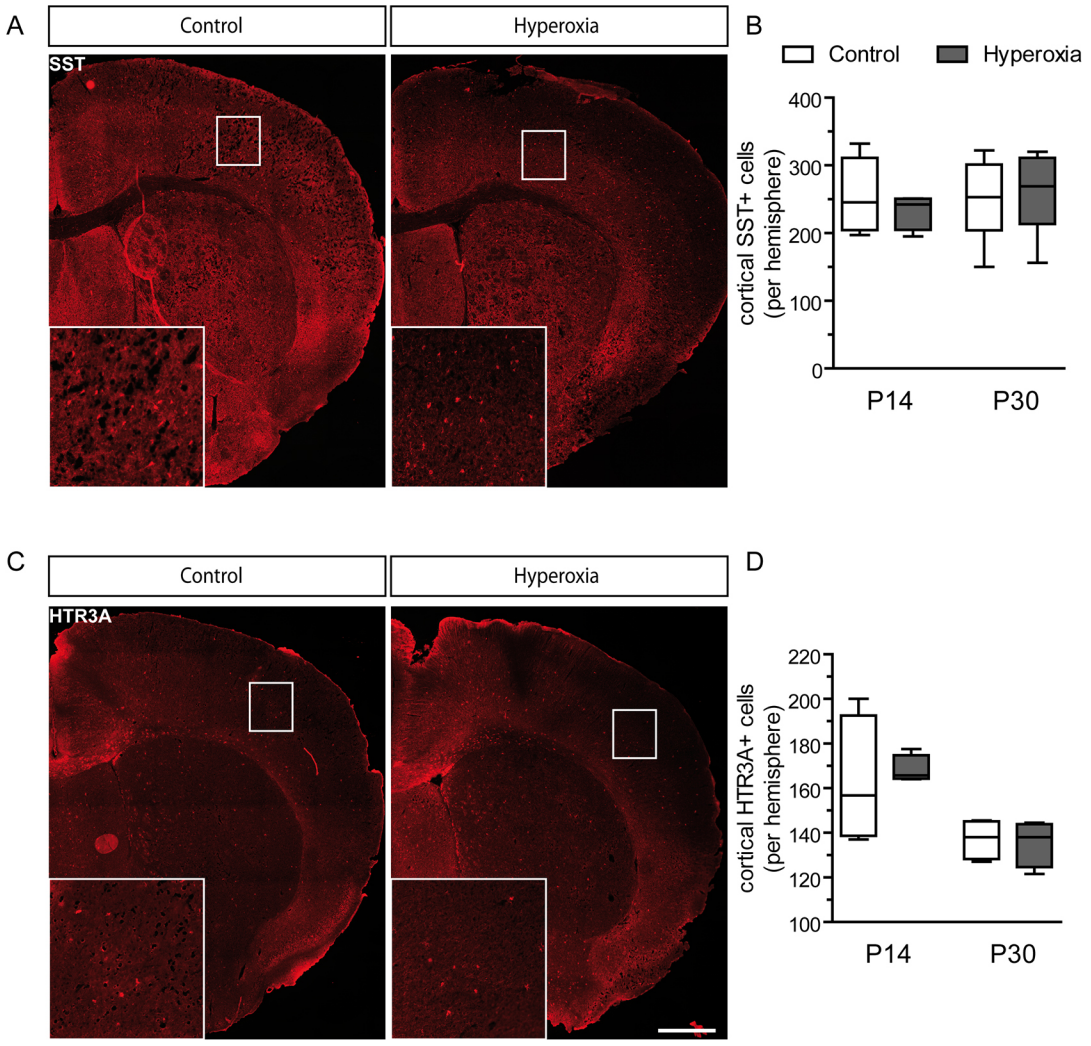

Fig. 4. Numbers of SST$^+$ and HTR3A$^+$ interneurons in the mouse cortex. (A,C) Immunohistochemical staining for SST (A) and HTR3A (C) of 10 µm coronal brain sections obtained from mice after 48 h neonatal hyperoxia (P5-P7) and controls at P14 and P30. Insets show the areas outlined at higher magnification. (B) Number of SST$^+$ interneurons, representing the second subgroup of cortical GABAergic interneurons derived from the medial ganglionic eminence was not affected by hyperoxia at the ages P14 and P30. (D) All GABAergic interneurons derived from the caudal ganglionic eminence express the 5-hydroxytryptamine receptor 3 A (HTR3A), representing all RELN$^+$ and VIP$^+$ interneurons. At P14 and P30, number of HTR3A$^+$ interneurons was not affected by hyperoxia exposure from P5 to P7 (n=4). Scale bar: 500 µm. White bar, control; black bar, hyperoxia. The line in the center of the box plot indicates the median. Whiskers indicate the minimum and maximum.

gene expression analysis was obtained for *Atg3* and *Atg12* by qPCR (Fig. 6C,D). At the ages P7-P14, there was no increase of autophagy detectable after neonatal exposure to hyperoxia. Microglial activation can affect interneuron development and may result in decreased interneuron density (Lacaille et al., 2019). To identify microglial activation as a possible cause of interneuronal damage, we performed immunohistochemical staining for IBA1 of the immature mouse cortex and analyzed cortical tumor necrosis factor α (*Tnf*) and interleukin 1 β (*Il1b*) RNA expression. As a result, we did not detect signs of increased microglial activity after exposure to hyperoxia in newborn mice at ages P7 and P9 (Fig. S1).

No impairment of mature PVALB$^+$ interneurons in patch-clamp analysis and morphology

In order to describe possible changes of electrophysiological properties in PVALB$^+$ interneurons as a consequence of neonatal oxidative stress, we applied patch-clamp analysis in transgenic VGAT-YFP-mice after exposure to 48 h hyperoxia (from P5-P7) in comparison with normoxic controls. At P23, when the expression of PVALB in mouse cortical interneurons can be observed in all cortical layers (Alcántara et al., 1996), electrophysiological properties such as maximal firing, the amplitude, the input resistance or the resting membrane potential of cortical PVALB$^+$YFP$^+$ interneurons were not affected by neonatal hyperoxia (Fig. 7A,B,D). For further morphological assessment, Sholl analysis, and length of axons and basal dendrites, as important morphological and functional features of PVALB$^+$ interneurons were determined, which did not show any changes in the hyperoxic animals (Fig. 7C, Fig. S2).

Hyperoxia induces cortical white matter injury with altered oligodendroglial GDNF secretion

Hyperoxia and oxidative stress induced white matter injury has been demonstrated in various studies, and white matter injury has recently been found to evoke interneuronal maldevelopment (Schmitz et al., 2011, 2014; Serdar et al., 2016; Stolp et al.,

Development (2021) 148, dev198390. doi:10.1242/dev.198390

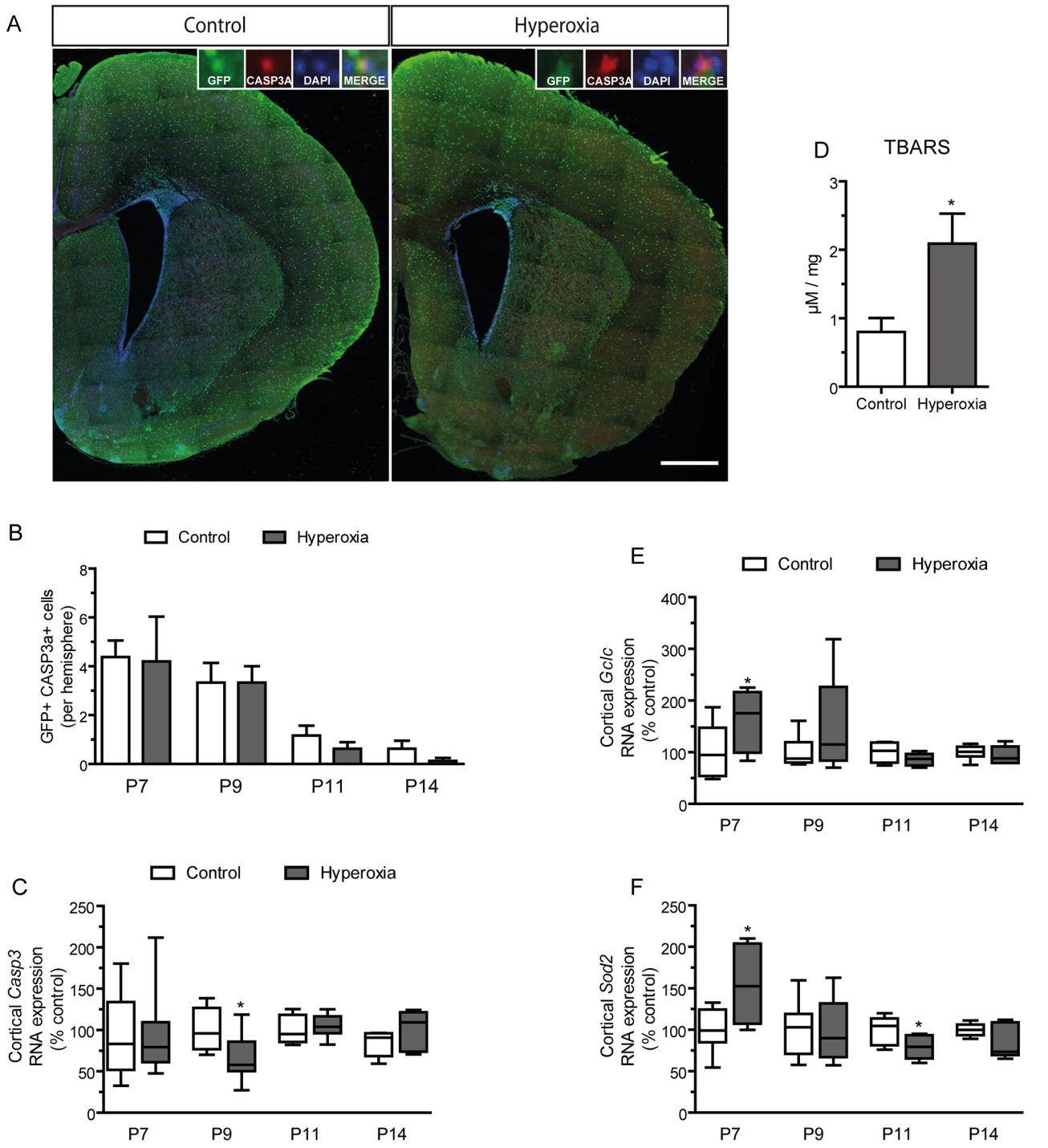

Fig. 5. Cell death of GABAergic interneurons in the cortex and oxidative stress in the mouse brain after exposure to hyperoxia. (A) Coronal brain sections (10 µm) from transgenic GAD67-EGFP mice were stained for CASP3A to detect cell death of cortical GABAergic interneurons at P7, P9, P11 and P14. Scale bar: 500 µm. (B) Hyperoxia exposure from P5 to P7 did not alter the number of $GFP^+CASP3A^+$ GABAergic interneurons at any time point [n=3 (P7, P9, P14), 4 (P11)]. (C) qPCR analyses of *Casp3* expression of cortical samples at P7, P9, P11 and P14 confirmed that no increase in cell death was detectable after hyperoxia exposure. However, at P9, gene expression of *Casp3* was decreased in cortical samples of animals exposed to hyperoxia (66%±11%). (D) TBARS assay to analyze lipid peroxidation detected an enhancement of oxidative stress in hyperoxia mouse brains at P7 (control=0.8±0.2 µM/mg versus hyperoxia=2.1±0.4 µM/mg) (for ELISA: n=8; t-test: *P<0.05). (E,F) Gene expression analysis of glutamate-cysteine ligase catalytic subunit (*Gclc*) (E) and superoxide dismutase 2 (*Sod2*) (F) at P7, P9, P11 and P14 reflected increase oxidative stress response in cortical samples. At P7, RNA expression of *Gclc* (162%±21%) and *Sod2* (154%±16%) was increased. However, *Sod2* (79%±6%) expression was decreased at P11 in the hyperoxia group [for qPCR: n=8 (P7), 7 (P9), 6 (P11-P14); t-test, Mann–Whitney U-test: *P<0.05]. White bar, control; black bar, hyperoxia. The line in the center of the box plot indicates the median. Whiskers indicate the minimum and maximum.

2019). To confirm that oligodendroglia injury also occurs in the cortex, we analyzed cortical gene expression of the oligodendroglia transcription factor *Olig2* and the maturation factor 2′,3′-cyclic-nucleotide 3′-phosphodiesterase (*Cnp*) (Fig. 8A,B). At P7, P9 and P14, gene expression of *Olig2* and *Cnp* was significantly reduced in the cortex of hyperoxia animals but returned to control level at P30

Development (2021) 148, dev198390. doi:10.1242/dev.198390

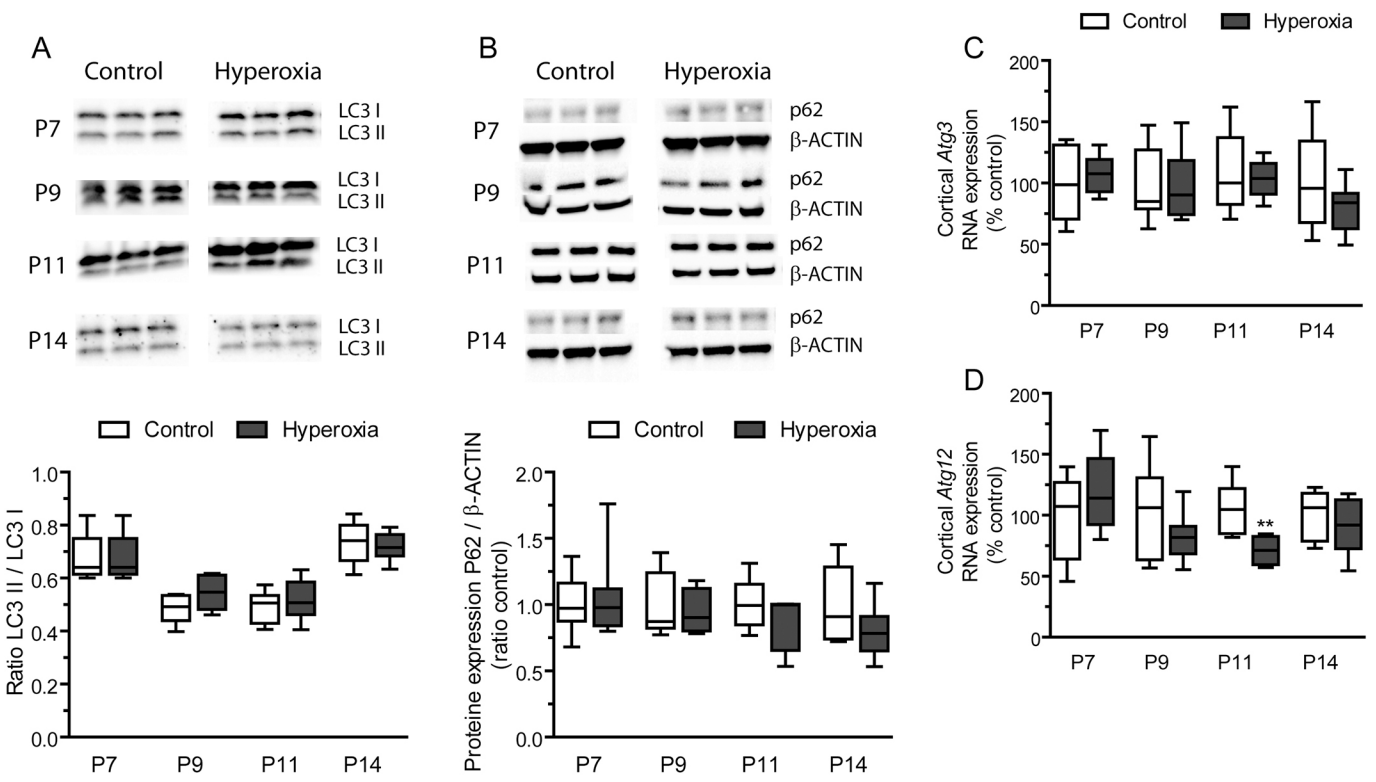

Fig. 6. Autophagy in the immature mouse cortex. (A-D) To analyze the impact of hyperoxia on autophagy at P7, P9, P11 and P14, western blots of microtubule-associated protein light chain 3 (LC3) and of sequestosome 1, also known as ubiquitin-binding protein p62 (p62), as well as qPCR analysis of autophagy-related gene 3 (*Atg3*) and *Atg12* were performed. For LC3 activity analysis, the ratio of the active membrane-bound form LC3 II and the cytosolic form LC3 I (LC3 II/LC3 I) was determined. (A) At all time points, there was no altered autophagy in cortical samples of mice exposed to neonatal hyperoxia. (B) Levels of p62 were normalized by β-actin expression. At all time points, p62 expression did not reveal any influence of hyperoxia on autophagy in the cortex (for western blots n=6). (C,D) RNA expression of *Atg3* (C) and of *Atg12* (D) confirmed no hyperoxia-induced alteration of autophagy in the cortex at P7, P9 and P14. However, expression of *Atg12* was decreased by earlier hyperoxia at P11 (71%±4%) [for qPCR: n=8 (P7), 7 (P9), 6 (P11-P14); t-test: $^{**}P$<0.01]. White bar, control; black bar, hyperoxia. The line in the center of the box plot indicates the median. Whiskers indicate the minimum and maximum.

(Fig. 8A,B). To verify in our cortical experiments the findings of previous studies on subcortical white matter, including myelin deficits after hyperoxia (Ritter et al., 2013), we quantified myelin basic protein (MBP) expression by western blot in cortical samples (Fig. 8C). At P9, P11 and P14, decreased protein expression of MBP in the cortex revealed diminished myelin production (Fig. 8D). At P30, MBP expression returned to control level.

Neuronal development and survival can be regulated by oligodendrocytes. For example, glial cell line-derived neurotrophic factor (GDNF) synthesized by oligodendrocytes is supporting neuronal development and maturation (Wilkins et al., 2003). In the mouse cortex, GDNF is expressed in OPCs and newly generated oligodendroglia (Pöyhönen et al., 2019). In our immunohistochemical co-staining for GDNF and OLIG2, we identified oligodendrocytes as a source of GDNF expression in the immature mouse cortex (Fig. 9A). RNA expression analysis documented a decrease in cortical *Gdnf* expression after exposure to hyperoxia at the age P7 and after 4 days of recovery at P11 (Fig. 9B). Given the pronounced variability of RNA expression in both the control group and hyperoxia group, we also performed western blot analysis at P7, P9, P11 and P14 (Fig. 9C). At all time points, western blot results confirmed a marked decrease in GDNF protein expression in the mouse cortex after hyperoxia (Fig. 9D). To verify oligodendroglial origin of the decrease in GDNF expression after exposure to hyperoxia, we analyzed GDNF protein levels *in vitro* in cultured cells of the oligodendroglia cell-line OLN93 after incubation at 80% O_2 or 21% O_2 for 48 h (Fig. 9E). As a result, the cell culture experiments verified that oligodendroglial lineage cells represent a source of GDNF being downregulated by increased oxygen exposure. Western blot analysis reveals decreased GDNF expression in OLN93 cells exposed to 80% O_2 (Fig. 9F). To highlight impaired GDNF signaling as a possible source of interneuronal maldevelopment, we investigated GDNF receptor α 1 (GFRα1) expression of PVALB$^+$ GABAergic interneurons in the postnatal cortex by immunohistochemistry at P14. Most of the PVALB$^+$ interneurons in the cortex express GFRα1 (Fig. 9G). However, GFRα1 expression is not limited to PVALB$^+$ interneurons.

Impaired learning and memory in mice exposed to hyperoxia

In recent studies, the involvement of PVALB$^+$ cortical interneuron activity in learning and memory consolidation was highlighted (Tripodi et al., 2018; Xia et al., 2017). To analyze the impact of the observed reduction of cortical PVALB-expressing interneurons on learning and memory, we performed the switched and the novel object test. All mice were habituated to four different objects in two exploration trials (Fig. 10C). For the third trial, two known objects were switched with each other (switched object test). The time spent with the two switched objects was compared with the time spent with the non-switched objects, both in correlation with the time spent with the objects in the previous trial. In the fourth trial, a known object was substituted for a new object (novel object trial). The time spent with the novel object was compared with the time spent with the known objects, both in correlation with

Development (2021) 148, dev198390. doi:10.1242/dev.198390

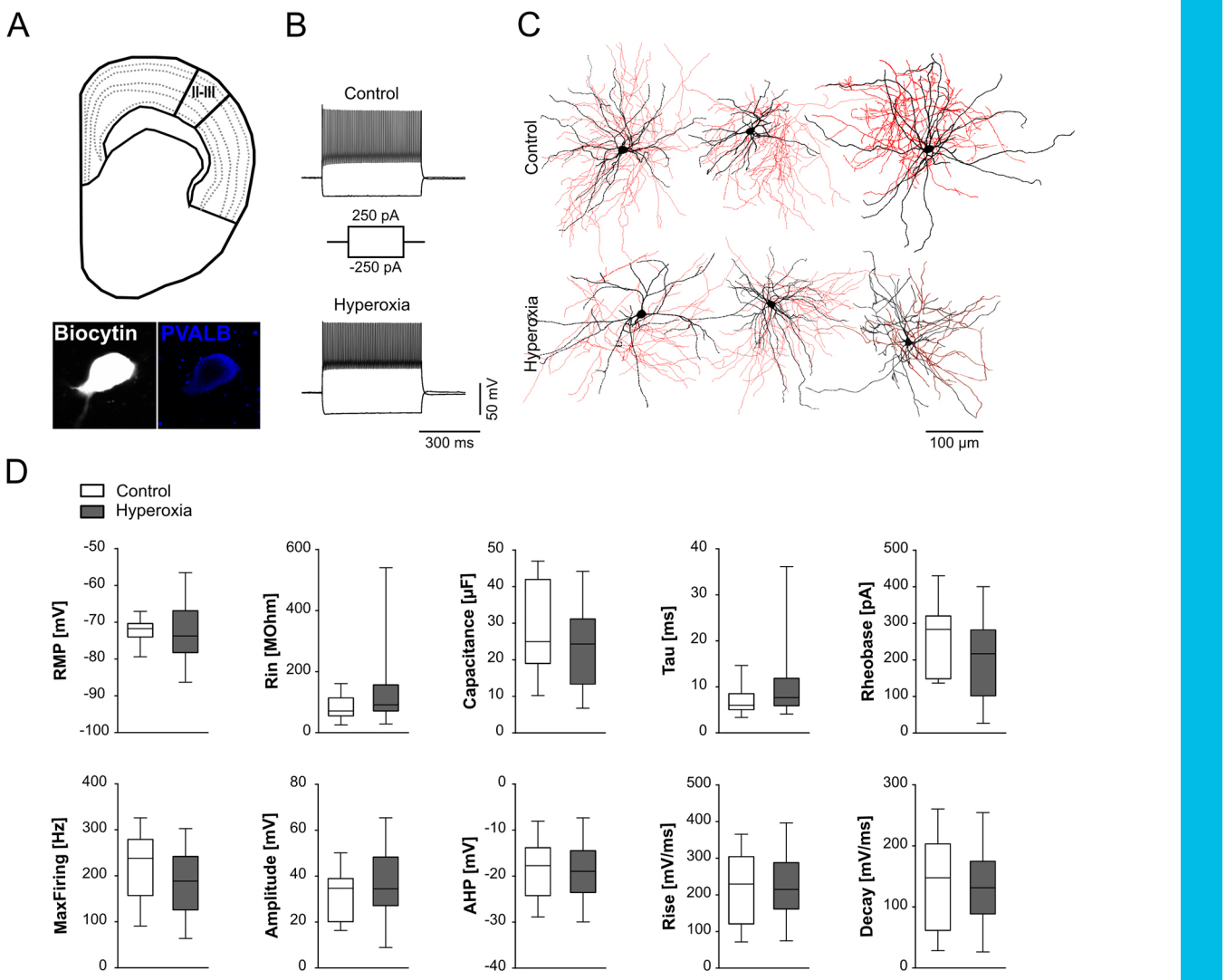

Fig. 7. Electrophysiological measurements in cortical PVALB$^+$ GABAergic interneurons. (A,B,D) Patch-clamp recording in cortical PVALB$^+$ GABAergic interneurons did not indicate any differences in resting membrane potential (RMP), input resistance (Rin), capacitance, the membrane time constant (Tau), rheobase, the maximum firing (MaxFiring), the amplitude, the after-hyperpolarization (AHP), rise and decay. (C) Morphological imaging of PVALB$^+$ GABAergic interneurons [control n=7 (12 PVALB$^+$ interneurons), hyperoxia n=12 (25 PVALB+ interneurons)]. White bar, control; black bar, hyperoxia. The line in the center of the box plot indicates the median. Whiskers indicate the minimum and maximum.

the times spent with the objects in the previous trial. As a result, animals exposed to neonatal hyperoxia showed no significant differences in exploring switched or novel objects compared with known objects at P60-P70 (Fig. 10A,B). Notably, this stands in clear contrast to the behavior observed in control animals, which spent significantly more time to explore the newly introduced or changed objects (Fig. 10A,B). Hence, neonatal exposure to hyperoxia abolished the ability to properly respond to novelty at young adult ages.

Early cerebral oxidative challenge resulted in altered social behavior in young adult mice

The function of PVALB$^+$ GABAergic interneurons is involved in establishment of functional social behavior and social interaction (Bicks et al., 2020). Poor social/interactive skills are one of the most common behavior problems in individuals born prematurely, and symptoms of autism spectrum disorders during childhood are largely increased and have been described in up to 8% of the children born prematurely (Arpi and Ferrari, 2013; Johnson et al., 2010). Moreover, pathologies of PVALB$^+$ interneurons were associated with schizophrenia-like symptoms (Jiang et al., 2013). To identify changes in the social behavior in mice caused by postnatal oxidative stress, we performed the sociability test and the social proximity test at age P60 (Fig. 11A-G). In the sociability test, which is a test of social interaction, hyperoxia-exposed mice did not show the same preference for interacting with an unfamiliar mouse as was observed in control mice (Fig. 11A,B). In the social proximity test, which is a test of social avoidance, social interaction (nose-to-head contact and nose tip-to-nose tip contact) of hyperoxia-exposed mice to an unfamiliar mouse was reduced prematurely compared with controls (Fig. 11D,E). To test for behavioral changes in mice indicating schizophrenia symptoms as a possible confounding reason for observed deficits in social interactions, we performed the prepulse inhibition (PPI) test. However, the results of the PPI test did not indicate impairments in sensori-motor gating in hyperoxia-exposed animals (Fig. 11H). Although ASD patients show an increased anxiety in unfamiliar environments (American Psychiatric Association and American

Development (2021) 148, dev198390. doi:10.1242/dev.198390

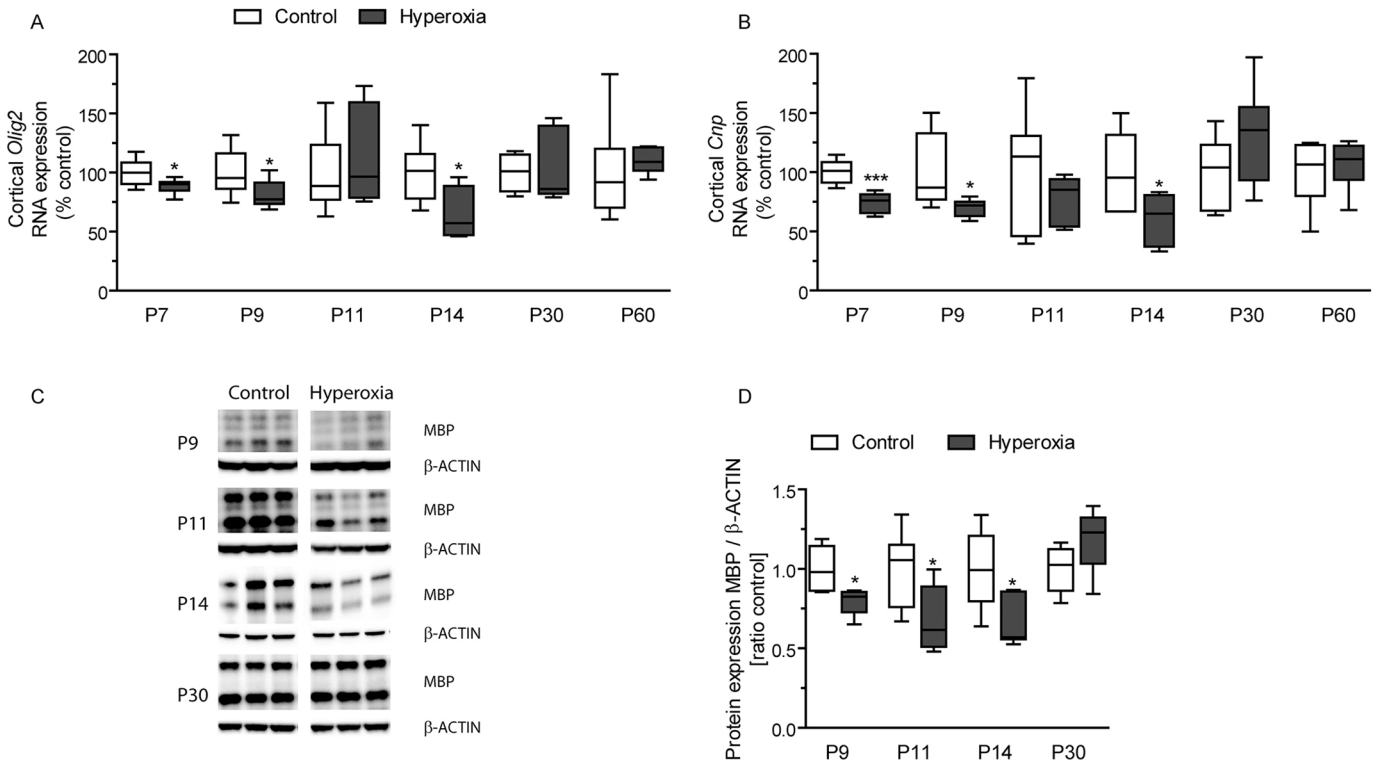

Fig. 8. Delayed cortical myelination after exposure to hyperoxia. (A,B) Real-time PCR analysis of the oligodendrocyte marker *Olig2* (A) and maturation marker *Cnp* (B) at P7, P9, P11, P14, P30 and P60. (A) Cortical *Olig2* RNA expression was significantly reduced at P7 (88%±2%), P9 (81%±4%) and P14 (66%±10%), and returns to control level at P30. (B) Expression analysis of *Cnp* reveals impaired maturation of cortical oligodendrocytes at P7 (74%±3%), P9 (70%±3%) and P14 (60%±10%) [for qPCR: n=8 (P7), 7 (P9), 6 (P11-P60), t-test, Mann–Whitney U-test *P<0.05; ***P<0.001]. (C,D) Western blot analyses of cortical samples indicated decreased MBP expression at P9 (0.79±0.03), P11 (0.68±0.08) and P14 (0.66±0.06). At P30, MBP expression was similar in both groups (for western blots: n=6; t-test, Mann–Whitney U-test: *P<0.05). White bar, control; black bar, hyperoxia. The line in the center of the box plot indicates the median. Whiskers indicate the minimum and maximum.

Psychiatric Association, 2013; Strang et al., 2012), hyperoxia-exposed animals did not show any symptoms of increased anxiety in two behavioral tests: elevated plus maze (Fig. 12A-I) and open field test (Fig. 12J-N).

DISCUSSION

In our experiments using the hyperoxia mouse model of preterm birth brain injury, neonatal oxidative stress caused pathologies of the GABAergic interneuronal cell population at juvenile and at adult ages, which was documented by reduced cortical RNA expression of *Lhx6* and *Pvalb*, and by markedly diminished density of mature PVALB-expressing interneurons in the cortex expanding from postnatal to young adult ages. In extension to the previously described developmental delay of the white matter, oligodendroglia impairment was documented in our experiments not only by diminished MBP production but also by decreased oligodendroglia-derived GDNF expression. Therefore, poor performance in the behavioral tests for recognition and memory, as well as impaired social interaction with peers, might be due to the interneuronal changes in mice after the neonatal hyperoxic challenge. As an underlying mechanism of cellular damage, we propose here that an increase in lipid peroxidation is an important oxidative stress indicator.

During fetal and early postnatal development, the brain undergoes dynamic processes of neuronal and interneuronal network establishment (Jiang and Nardelli, 2016; Vasung et al., 2019). Starting from the third trimester of gestation and extending for several months after birth, crucial steps of migration and maturation influence the fate and the functionality of GABAergic interneurons, as well as the GABAergic inhibitory network in the cortex, which is finally modulating neuronal and axonal signal transmission (Hu et al., 2014; Jovanovic and Thomson, 2011; Kilb, 2012). A pronounced susceptibility of GABAergic interneurons during early brain development to external stimuli has been characterized in human studies in response to perinatal inflammation (Vasistha et al., 2019), prenatal stress (Lussier and Stevens, 2016) and preterm birth (Panda et al., 2018; Stolp et al., 2019).

In the cortex, inhibitory GABAergic interneurons are modifying and directing neuronal activity, and interneuronal dysfunction is acknowledged to play an important role in the etiology of several psychiatric diseases, including ADHD (Wang et al., 2012) and ASD (Gao and Penzes, 2015; Hashemi et al., 2017). Oxidative stress can cause cellular damage of GABAergic interneurons, leading to decreased neuronal activity (Sakurai and Gamo, 2019). In adult patients with ADHD, cortical GABA levels measured by magnetic resonance spectroscopy were lower in comparison with healthy control individuals (Edden et al., 2012), complementing the concept of interneuronal deficits being involved.

The relevance of the GABA network for psychiatric diseases has also been underlined by studies in adult mice with a genetic knockout of the GABA transporter subtype 1, which developed symptoms of motor hyperactivity and ADHD (Yang et al., 2013). In animal studies, reduction of $PVALB^{+}$ interneuron number or PVALB expression has been linked to ASD symptoms (Filice and Schwaller, 2017), and energy deficit in $PVLAB^{+}$ interneurons

Development (2021) 148, dev198390. doi:10.1242/dev.198390

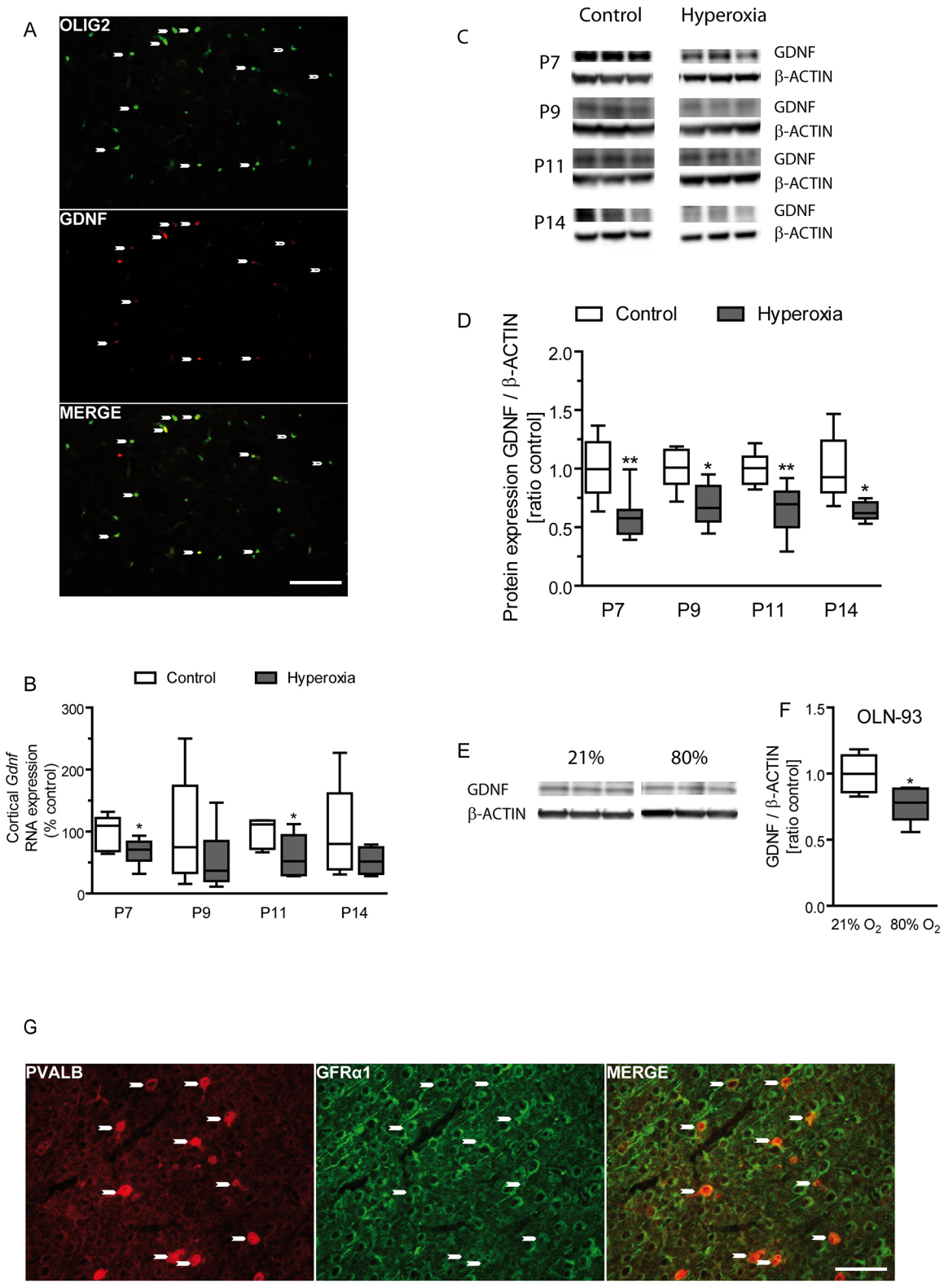

Fig. 9. Neonatal oxygen exposure impairs oligodendroglial GDNF expression. (A) Immunohistochemical staining of 10 µm coronal section for oligodendrocyte marker OLIG2 and GDNF confirmed GDNF expression in cortical oligodendrocytes. Arrowheads indicate OLIG2^{+}GDNF^{+} oligodendrocytes. (B) Real-time PCR analysis at P7, P9, P11 and P14 indicated decreased cortical expression of GDNF at P7 (67%±7%) and P11 (60%±14%) in hyperoxia-exposed animals [for qPCR: n=8 (P7), 7 (P9), 6 (P11-P14); t-test: *P<0.05]. (C,D) Western blot analysis of cortical samples confirmed decreased expression of GDNF at P7 (0.6±0.06), P9 (0.69±0.07), P11 (0.66±0.09) and P14 (0.64±0.03) in hyperoxia-exposed animals (for western blots: n=6; t-test: *P<0.05; **P<0.01). (E,F) Western blot analyses of OLN93 cells incubated in 80% oxygen and 21% oxygen (E) reveals decreased GDNF expression in oligodendroglial lineage cells at higher oxygen concentrations (F) (for western blot: n=6; t-test: *P<0.05). (G) Immunohistochemical staining of 10 µm coronal section for GDNF receptor α 1 (GFRα1) and PVALB at P14. Arrowheads indicate PVALB^{+}GFRα1^{+} interneurons. Scale bars: 200 µm. White bar, control; black bar, hyperoxia. The line in the center of the box plot indicates the median. Whiskers indicate the minimum and maximum.

Development (2021) 148, dev198390. doi:10.1242/dev.198390

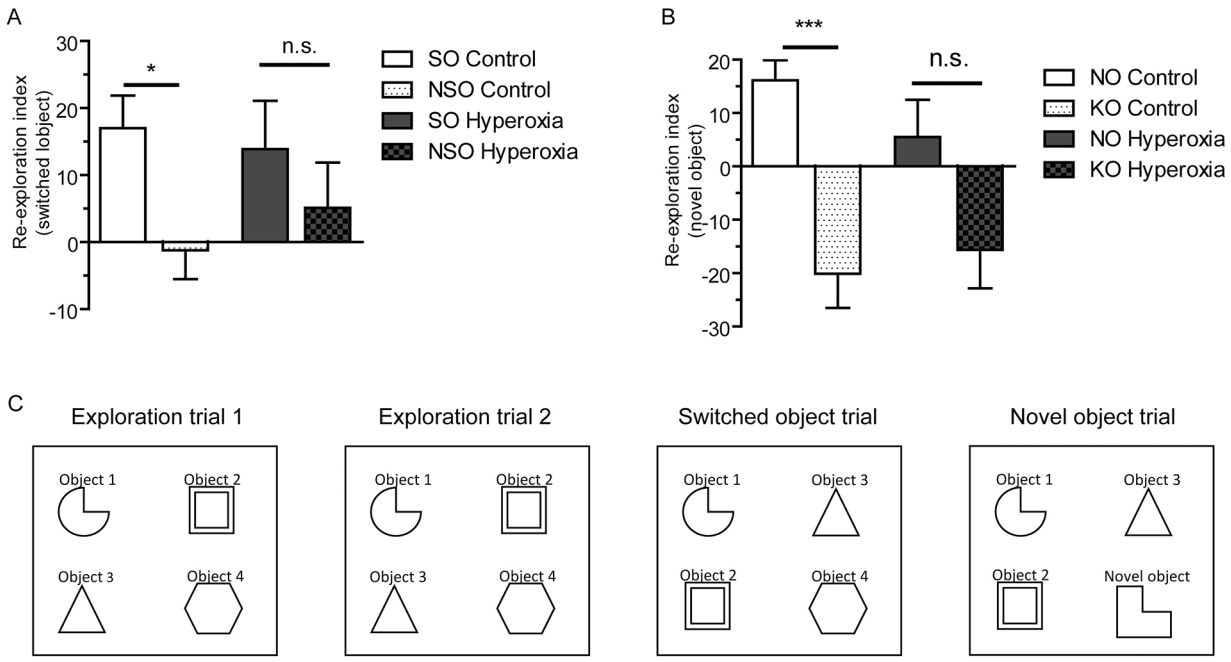

Fig. 10. Object recognition test in young adult mice. (C) In the novel object and the switched object recognition test, after an open field trial, P60 mice were first habituated to four different objects in two consecutive exploration trials. In the switched object trial (third trial), two of the known objects were swapped with each other. In the novel object trial (fourth trial), one of the known objects was replaced with a novel unknown object. (A,B) The objects were classified in different groups as switched objects (SO), non-switched objects (NSO), novel object (NO) and known objects (KO). The ability of the animals to selectively react to the spatial change was analyzed by calculating the spatial re-exploration index based on the exploration time: SO (trial 3)-SO (trial 2)=SO; NSO (trial 3)-NSO (trial 2)=NSO; NO (trial 4)-NO (trial 3)=NO; KO (trial 4)-KO (trial 3)=KO. (A) In the switched object trial, control animals significantly recognized the swapping of the two objects (17±5 versus −1±4). Hyperoxia-exposed animals did not recognized the swapping of the two objects (14±7 versus 5±7). (B) In the novel object trial, control mice clearly identified the novel object (16±3.5 versus −20±6.5). No significant signs of novel object recognition were observed in hyperoxia-exposed mice (5.5±7 versus −15±7) (control, n=8; hyperoxia, n=9, t-test: *P<0.05; ***P<0.001). White bar, control; black bar, hyperoxia.

caused impaired social interaction (Inan et al., 2016). Moreover, mice with Pvalb knockout display behavioral phenotypes of ASD with relevance to core symptoms in humans: abnormal reciprocal social interactions, impairments in communication, and repetitive and stereotyped patterns of behavior (Wöhr et al., 2015).

A role of oxidative stress for interneuronal impairment was demonstrated by Cabungcal and co-workers, who exposed Gclm knockout mice with genetically downregulated anti-oxidant capacity to oxidative challenges using a pharmacological approach (Cabungcal et al., 2013). However, a behavioral phenotype resulting from the interneuronal damage was not the subject of that study.

In our current experiments, the expression of interneuronal markers *Sst*, *Reln* and *Vip* was transiently affected by exposure to neonatal oxidative stress and returned back to control levels a few days after recovery in room air. Gene expression analysis and immunohistochemistry did not reveal persistent changes in these subpopulations. In contrast, alterations of SST^+ interneuronal numbers or marker expression has been reported to coincide with depressive-like behaviors (Girgenti et al., 2019; Lin and Sibille, 2013). In humans, a reduction of SST^+ interneurons in the upper cortical layers can be caused by preterm birth (Lacaille et al., 2019). Instead, the deficits in the gene expression of *Lhx6* and *Pvalb* in cortical samples persisted for longer times after the oxidative challenge, and a marked loss of mature PVALB-expressing interneurons was maintained until adult ages, as confirmed by western blot and immunohistochemistry in the cortex. Additionally, long-term recovery of cortical SST^+, $RELN^+$ and VIP^+ interneurons could also be demonstrated by immunohistochemistry and western blot.

So far, the origin of psychiatric disorders related to pathologies of the cortical GABAergic system has mostly been linked to abnormalities in $PVALB^+$ interneurons (Ferguson and Gao, 2018). In our experiments in mice, the loss of PVALB-expressing interneuronal cells after hyperoxia could not be explained by overt signs of increased autophagy in hyperoxic wild-type mice or by increased apoptotic cell death in the GAD67-EGFP mice. However, in theory, apoptosis could have occurred at earlier time points during exposure to hyperoxia and might have affected immature $PVALB^+$ interneurons. Theoretically, postnatal maturation of parvalbumin-expressing interneurons was interrupted by oxidative stress. Redox dysregulation during postnatal development disables parvalbumin expression in $PVALB^+$ interneurons with a loss of function in different models of schizophrenia (Powell et al., 2012). Potentially, a lack of or incomplete maturation of $PVALB^+$ interneurons can also result from altered interneuron-glia interaction during brain development. In a previous study, we showed that neonatal hyperoxia and oxidative stress is causing white matter pathologies, including delayed oligodendroglial maturation and hypomyelination (Schmitz et al., 2011), which was confirmed for the cortex in this study. White matter damage has been found to coincide with a reduced number of cortical GABAergic interneurons in humans and in animal models of preterm birth brain injury (Stolp et al., 2019). Oligodendrocytes provide electric isolation and metabolic support for GABAergic interneurons, and $PVALB^+$ interneurons have the highest myelination proportion of all GABAergic interneurons. The development of immature interneurons and oligodendrocyte precursor cells occur interactively in the immature cortex (Benamer et al., 2020; Orduz et al., 2015), and disturbed crosstalk between these cells may

Development (2021) 148, dev198390. doi:10.1242/dev.198390

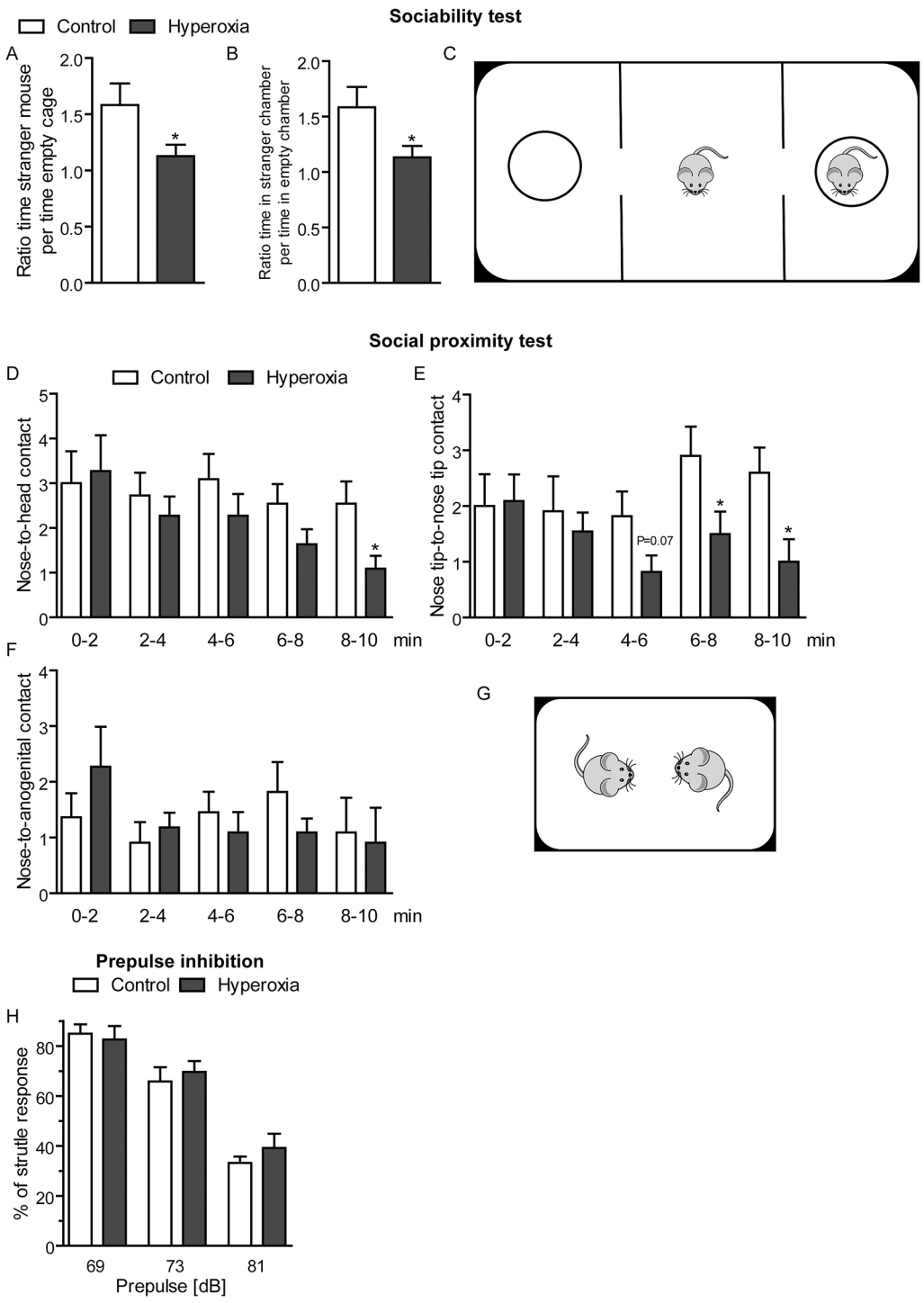

Fig. 11. Social behavior of young adult mice. (C,G) Social interaction of P60 mice was observed by the sociability test and the social proximity test. In the sociability test, the preference of the mouse to interact with an unfamiliar mouse was analyzed in a tripartite chamber, which is composed of three chambers of equal size; two cylindrical cages, one empty and one containing the unfamiliar mouse, were placed in the lateral chambers. (A) After 10 min, the preference for interacting with the unfamiliar mouse when compared with the empty cage was determined by the ratio of time spent with the unfamiliar mouse over the time spent with the empty cage. Hyperoxia-exposed mice did not show a preference for interacting with the unfamiliar mouse. The ratio of time interacting with the mouse peer over time spent with the empty cage was decreased (control=1.6±0.2 versus hyperoxia=1.1±0.1). (B) In a similar way, the ratio of time spent in the unfamiliar mouse chamber by time spent in the empty chamber was decreased in hyperoxia-exposed animals (control=1.6±0.2 versus hyperoxia=1.1±0.1) (control, n=8; hyperoxia, n=9, t-test: *P<0.05). (G) The social proximity test provides a sub-analysis of behavior in a situation in which the focus is not on avoidance of peer animals but instead on characteristics of interaction during contact. For 10 min, interactions with an unfamiliar mouse were analyzed in a testing cage (7 cm×14 cm). (D) After 8 min, hyperoxia-exposed animals significantly reduced the nose-to-head contact with the unfamiliar mouse (control=2.5±0.5 versus hyperoxia=1.1±0.1). (E) A reduction of the nose tip-to-nose tip contact occurred at much earlier time points: there was a tendency towards decreased contact after 4 min (P=0.07, control=1.8±0.4 versus hyperoxia=0.8±0.3), and nose tip-to-nose tip contact was significantly reduced after 6 min (control=2.9±0.5 versus hyperoxia=1.5±0.4) and 8 min (control=2.6±0.4 versus hyperoxia=1.0±0.4) (t-test: *P<0.05). (F) Interaction by nose-to-anogenital contact was not affected by hyperoxia (n=11, t-test: *P<0.05). (H) A prepulse inhibition (PPI) test to measure sensorimotor gating was performed in a standard startle chamber. PPI did not reveal any change in startle or reflex response (control, n=8; hyperoxia, n=9). White bar, control; black bar, hyperoxia.

Development (2021) 148, dev198390. doi:10.1242/dev.198390

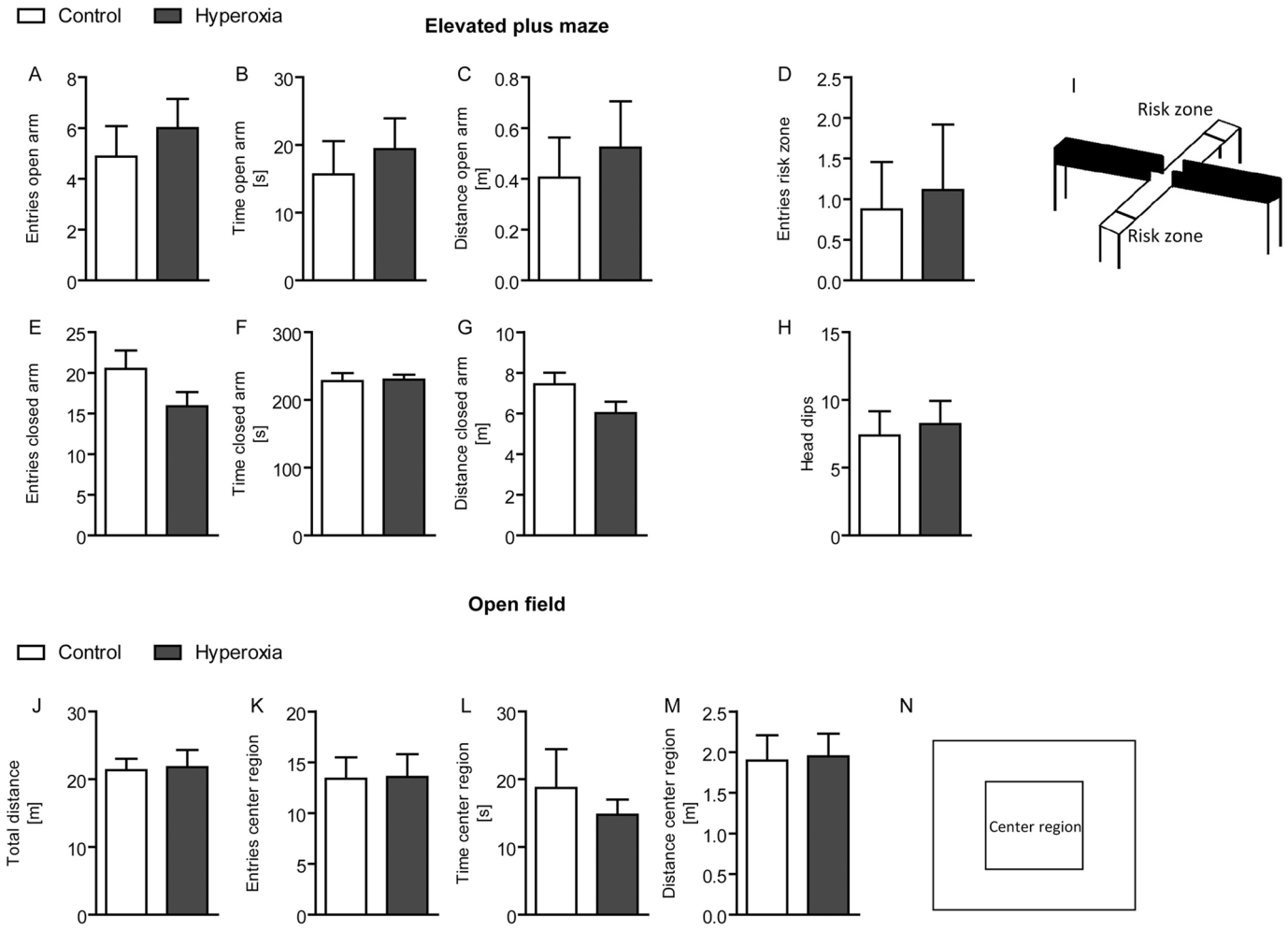

Fig. 12. Investigation of anxiety behavior in young adult mice. (I,N) The elevated plus maze (I) and the open field test (N) were performed to study anxiety behavior in P60 mice. In the elevated plus maze test, hyperoxia-exposed mice did not show altered anxiety. (A-H) There was no difference in the number of entries to the open (A) or closed arms (E), in the time spent in the open (B) or closed arms (F), in the distance walked in the open (C) or closed arms (G), in the number of entries into the risk zone (D) or in head dips (H) compared with control animals. (J-L) In the open field test, anxiety behavior of control and hyperoxia-exposed animals was equal. There was no difference in total distance walked (J), or in the time spent in (K), in entries into (L) or in distance walked into (M) the center region (control, *n*=8; hyperoxia, *n*=9). White bar, control; black bar, hyperoxia.

represent the cellular basis of brain pathology in schizophrenia (Raabe et al., 2019). We identified decreased oligodendroglial GDNF expression as a consequence of postnatal hyperoxia. GDNF function is involved in migration, differentiation and maturation of MGE-derived cortical GABAergic interneurons (Canty et al., 2009; Pozas and Ibáñez, 2005). Hence, the loss of the cortical PVALB$^+$ interneuron population in our study may occur in close relation to oligodendroglial damage in hyperoxic mice, which is mediated by reduction of oligodendroglial GDNF.

Neurotransmitter signaling, such as GABA release, is important for developmental processes through the regulation of intracellular calcium, which is required for many cellular functions, i.e. cytoskeletal remodeling (Manent and Represa, 2007), and GABA signaling is indispensable for oligodendroglia development (Habermacher et al., 2019). Bi-directional damage as a secondary consequence, caused by decreased numbers of mature parvalbumin-expressing interneurons, might enhance the damage in cortical oligodendroglia after previous exposure to oxidative stress. White matter alteration might also interfere with deficits in learning and cognition, and could contribute to the development of psychiatric disorders, such as ADHD and autism (Fields, 2008). However, although myelin deficits and white matter damage are compensated for during long-term recovery in room air in this mouse model (Schmitz et al., 2011), the persistent changes in cortical PVALB$^+$ interneurons until the ages when behavior tasks were performed, i.e. interneuronal damage, can be regarded as an important cause of behavioral impairment.

In this study, ASD-like behavior was observed, characterized by a poor interest in peer animals and loss of interaction with unfamiliar mice. Marked learning deficits were revealed in the switched object and novel object tests. Our data extend the picture of an ADHD-like phenotype in the hyperoxia mice in line with a previous study in the same model showing motor hyperactivity and reduced motor learning at young adult ages (Schmitz et al., 2012). Although increased levels of anxiety and poor stress management are often reported as common concerns in preterm infants and in children with ASD (Johnson and Marlow, 2011; White et al., 2009), and silencing of PVALB$^+$ interneurons may contribute to anxiety-related neurological and psychiatric disorders (Panthi and Leitch, 2019), we did not discover signs of anxiety in our animals in the open field and the elevated plus maze test. The results from the PPI test did not reveal the presence of sensorimotor gating deficits in hyperoxia-exposed mice, which suggest

Development (2021) 148, dev198390. doi:10.1242/dev.198390

the lack of a schizophrenia-like phenotype. A reduced number of $PVALB^+$ interneurons has also been found in an animal model of schizophrenia (Lodge et al., 2009), and in NMDAR hypofunctional mice, increased oxidative stress was induced after maternal separation to aggravate schizophrenia-like symptoms (Jiang et al., 2013). Our environmental model is applied in wild-type mice without genetic manipulation of interneurons, and the extent of interneuronal damage might be less pronounced and may therefore not result in schizophrenia-like symptoms. The rather mild extent of brain injury in the hyperoxia model, though, closely resembles the subtle pathologies often seen in preterm infants. The translational value of our study is also strengthened by the fact that the shared features of ASD and ADHD found in our hyperoxia-exposed animals has also been obtained in human cohorts after preterm birth (Lake et al., 2019).

The results of our study show that the early increase in oxygen exposure largely and persistently reduces the number of mature PVALB-expressing GABAergic interneurons in the cortex and can be one of the causes leading to behavioral problems similar to the psychiatric symptoms often found in preterm infants. Impaired development of cortical interneurons may interact with the observed cortical white matter injury and could also be induced or enhanced by decreased oligodendrocyte-derived GDNF expression. Oxygen-induced oxidative stress therefore represents an early external factor that contributes to symptoms of psychiatric disorders in preterm infants and offers a potential target for future preventive and therapeutic strategies.

MATERIALS AND METHODS

Animal experiments

All animal experiments were performed with the permission of the Animal Welfare Committee of Berlin (G0084/11, G0151/14 and G0224/16). Wild-type mice (C57BL/6), transgenic VGAT-EYFP mice and GAD67-EGFP transgenic mice age P5 were exposed to 80% oxygen for 48 h together with their mothers in an OxyCycler chamber (OxyCycler BioSpherix). The animals recovered in room air for different times thereafter until analysis at ages P9, P11, P15, P23, P30 and P60. Behavioral analyses were performed at P60-P70.

Cell culture

We received cells of the oligodendroglia lineage cell line OLN93 (Richter-Landsberg and Heinrich, 1996) from Dr C. Richter-Landsberg (Oldenburg, Germany). Cells were cultured as described previously (Brill et al., 2017).

Briefly, for protein expression analyses, 1.5×10^6 cells per six-well plate were incubated at 80% and 21% oxygen. During oxygen exposure, cells were cultured with only 1% FCS and without any antibiotic, to avoid anti-oxidative stress effects of medium compounds. After a 48 h incubation, cells were harvested for western blot analysis.

Real-time PCR

Total cellular RNA was isolated from snap frozen tissue by acidic phenol/chloroform extraction (peqGold RNA–Pure, peqLab). Two µg of total RNA was reverse transcribed (M–MLV Reverse Transkriptase, Promega) after DNase (Qiagen) pre-treatment. The cDNA was analyzed with specific primers and probes for markers of the distinct GABAergic interneuronal subtypes (*Lhx6*, *Sst*, *Pvalb*, *Reln* and *Vip*), oligodendroglia (*Olig2* and *Cnp*), apoptosis (*Casp3*), autophagy (*Atg3* and *Atg12*), inflammation (*Tnfa* and *Il1b*), oxidative stress (*Gclc* and *Sod2*) and glia cell-derived neurotrophic factor (*Gdnf*) (Table S1). The expression of target genes was analyzed with the StepOnePlus Realtime PCR System (Applied Biosystems) according to the $2^{-\Delta\Delta CT}$ method (Livak and Schmittgen, 2001). Expression of the housekeeping gene *Hprt* was used as an internal reference.

Western blot

For western blotting, 20 µg of isolated protein was separated by electrophoresis using a 4-20% Criterion TGX Precast Mini/Midi Protein Gel (Bio-Rad). After electroblotting (Trans–Blot Turbo Transfer System, BioRad) to a nitrocellulose membrane and blocking of nonspecific binding sites (Roti–Block, Roth), membranes were exposed to primary antibodies: LC3 (Abcam, ab48394, 1:1000), SQSTM1/p62 (Abcam, ab91526, 1:1000), GDNF (Invitrogen, PA1-9524, 1:1000), MBP (Covance, SMI-99P, 1:1000), PVALB (Abcam, ab11427, 1:1000), SST (R&D Systems, MAB2358, 1:500), RELN (Millipore, MAB5364, 1:1000), VIP (ABclonal, A1804, 1:1000) and β-actin (Sigma, A5316, 1:5000) followed by appropriate secondary antibodies conjugated with horseradish peroxidase (donkey anti rabbit Pierce 31458, 1:5000; rabbit anti mouse Dako P0260, 1:5000; goat anti chicken Invitrogen A16054, 1:5000) and detection by chemiluminescence (PerkinElmer, USA). Loading control β-actin was used as an internal reference. For western blot, sample size depends on gel size.

Thiobarbituric acid reactive substances (TBARS) assay

Lipid peroxidation in whole-brain samples was determined using the TBARS assay kit (Cayman Chemical) according to the manufacturer's instructions. TBARS concentration was normalized to the total amount of protein.

Immunohistochemistry

Mice were anesthetized following German guidelines and transcardially perfused with PBS followed by 4% paraformaldehyde (PFA). Brains were dissected, post-fixed with 4% PFA at 4°C overnight before they were preserved in paraffin wax. Coronal brain sections were cut (10 µm) and stored on slides at room temperature. After removal of paraffin wax, fluorescence staining was performed for the GABAergic interneuron subtype markers parvalbumin (PVALB, Abcam ab11427, 1:1000), somatostain (SST, Atlas Antibodies, HPA019472, 1:1000) and serotonin receptor 3A (HTR3A, ABclonal, A5647, 1:200), as well as oligodendrocyte marker OLIG2 (R&D Systems, AF2418, 1:2000), GDNF (R&D Systems, MAB212, 1:100), GDNF receptor alpha 1 (GFRα1, R&D Systems, AF560, 1:100) and microglia marker IBA1 (Wako, 019-19741, 1:750). For HTR3A detection, signal amplification was performed with the TSA Plus Cyanine 3 kit (Perkin Elmer, NEL744001KT) according to the manufacturer's instructions. Brain slices from GAD67-EGFP mice were stained using anti-GFP antibody (Abcam, ab6673, 1:1000) and apoptosis marker cleaved caspase 3 (CASP3A, Cell Signaling, #9664, 1:200). After incubation with the primary antibodies, brain sections were incubated with the secondary antibodies Alexa Fluor 488 goat anti-rabbit IgG (Thermo Fisher Scientific A11034, 1:200), Alexa Fluor 594 goat anti-rabbit IgG (Thermo Fisher Scientific A11037, 1:200), Alexa Fluor 594 goat anti-mouse IgG (Thermo Fisher Scientific A11032, 1:200) and Alexa Fluor 488 donkey anti-goat IgG (Thermo Fisher Scientific A11055, 1:200). After the final incubation step, sections were mounted in Fluoroshield with DAPI (4′,6-diamidino-2-phenylindole, Sigma). For cell counting, two plane hemisphere sections (left and right) per animal were analyzed. Cell number of all layers in the frontal cortex were counted without layer distribution.

Microscope measurements

Immunohistochemically stained brain sections were analyzed using a Keyence compact fluorescent microscope BZ 9000 with a 10×, 20× and 40× objective, the BZ–II Viewer software and BZ–II Analyzer software (Keyence). The number of immunolabeled cells were determined using Photoshop CSM (Adobe). Merged images were processed in Photoshop CSM with minimal manipulation of contrast.

Acute cortical slice preparation

Acute brain slices were obtained from ∼23-day-old C57BL/6 VGAT-YFP mice by quickly removing brains after deep isoflurane (3%) anesthesia and transferring them into carbogenated (95% O_2/5% CO_2), ice-cold sucrose-ACSF (sACSF, in mM: 87 NaCl, 2.5 KCl, 25 $NaHCO_3$, 1.25 NaH_2PO_4, 25 glucose, 75 sucrose, 1 sodium pyruvate, 1 sodium ascorbate, 7 $MgCl_2$, 0.5 $CaCl_2$). Coronal brain slices (300 µm) were cut on a Vibratome (VT1200s; Leica), transferred to a submerged holding chamber containing carbogenated sucrose-ACSF at a temperature of 34°C, incubated for 30 min and subsequently stored at room temperature.

Development (2021) 148, dev198390. doi:10.1242/dev.198390

Whole-cell patch-clamp recordings

For electrophysiological patch-clamp recordings, slices were visualized using an infrared differential contrast illumination by means of an upright microscope (BX-50, Olympus) equipped with a 20× water-immersion objective. Whole-cell patch-clamp recordings were performed using a Multiclamp 700B amplifier (Molecular Devices). Recording pipettes were pulled from borosilicate glass capillaries (2 mm outer/1 mm inner diameter, Hilgenberg, Germany) on a horizontal electrode puller (P-97, Sutter Instruments) and filled with intracellular solution (in mM: 130 potassium gluconate, 10 KCl, 2 $MgCl_2$, 10 EGTA, 10 HEPES, 2 Na_2-ATP, 0.3 Na_2-GTP, 1 Na_2-creatinine and 0.1% Biocytin; 290-310 mOsm; pH 7.4). Voltage-clamp recordings were performed at a holding potential of −65 mV and all current-clamp recordings from the resting membrane potential at a sampling rate of 20 kHz were made on an analog-digital interface (Axon Digidata 1440A, Molecular Devices) and acquired with WinWCP software (courtesy of John Dempster, Strathclyde University, Glasgow, UK). Data were analyzed offline using the open source Stimfit software package (Guzman et al., 2014). Cells were recorded initially in current clamp and a family of depolarizing to hyperpolarizing current steps was injected (−250 to 450 pA, 500 ms duration) to determine intrinsic membrane properties and action potential discharge properties. At the end of each recording, the pipette was carefully removed from the cell to form an outside-out patch and the slice was fixed overnight in 0.1 M PB containing 4% PFA.

For histological staining, slices were incubated with primary antibody mouse anti-PVALB (SWANT, 235, 1:5000) and then incubated with secondary antibody goat anti-mouse Alexa Fluor 405 (Thermo Fisher Scientific A-31553, 1:500) and Alexa Fluor 647 conjugated streptavidin (Thermo Fisher Scientific S21374, 1:500). After the final washing step, slices were mounted on glass slides with a 300 µm metal spacer and mounting medium (Fluoromount-G, Southern Biotech).

Imaging and reconstructions

Image stacks were acquired on a confocal laser-scanning microscope (FluoView 1000; Olympus) using a 30× silicone oil-immersion objective (N.A. 1.05; Olympus) with a resolution of 1024×1024 and a step size of 0.8 µm. 3D reconstructions of $PVALB^+$ interneurons were generated from image stacks using Neutube (Feng et al., 2015) and subsequently analyzed using Neuron (Hines and Carnevale, 1997).

Behavioral analyses

For all behavioral analyses, only male animals were used. Open field test, switched object and the novel object recognition test, elevated plus maze test, sociability test and prepulse inhibition test were performed with the same number of animals and the same cohort of mice. Social proximity testing was performed in two separate cohorts.

Open field test

Mice show distinct aversions to large, brightly lit, open and unknown environments (Seibenhener and Wooten, 2015). The open field test was used to analyze anxiety-like behavior in the mice. In a square-shaped box with high walls (72×72×33 cm) made of white high density and non-porous plastic, mice were placed in the center region. For 5 min, the mice had the ability to explore the area. The behavior of the animals was recorded by a camera. Measurements were performed with anymaze software (ANY-maze 4.50, Stoelting Europe, Dublin, Ireland). Distance walked, time and entries in the center region were recorded.

The switched object and the novel object recognition test

The test was performed in a square-shaped open-field box with high walls (72×72×33 cm) as described previously (Mattei et al., 2017) with some modifications. Briefly, after 5 min open field trial, the mouse explored four different objects in two exploration trials (5 min each). Following the second exploration trial (trial 2), two of the known objects were displaced with each other. In this switched object trial (trial 3), the mouse explored the four different objects for 5 min again. In the last trial, the novel object trial (trial 4), one of the objects was replaced by a novel unknown object. In that final trial, the mouse explored the four objects for 5 min again. The behavior of the animals was recorded using a camera. Analysis was performed with anymaze software. In sessions four and five, objects were classified in different groups for switched objects (SO) and non-switched objects (NSO), as well as novel object (NO) and known objects (KO). The ability of the animals to selectively react to the spatial changes were analyzed by calculating the spatial re-exploration index based on the exploration time, as described by De Leonibus et al. (2009). SO (trial 3)−SO (trial 2)=SO and NSO (trial 3)−NSO (trial 2)=NSO; NO (trial 4)–NO (trial 3)=NO and KO (trial 4)–KO (trial 3)=KO.

The elevated plus maze test

The elevated plus maze test (EPM) is an animal test for anxiety-like behavior. The test apparatus is made of four equal arms in length and width. These arms form a plus sign shape radiating from a center platform with two opposed closed arms and two opposed open arms. The EPM is elevated from the bottom (Rodgers and Dalvi, 1997). For testing, a mouse was placed on the central platform, and behavior was recorded by a camera for 5 min. Measurements were performed with anymaze software. Head dips, entries into the risk zone, the time, entries and distance traveled in the open and closed arms were recorded.

Sociability test

Social behavior of the mice was analyzed by the sociability test as described elsewhere (Mattei et al., 2017). Briefly, after a 5 min habituation in the middle chamber of a tripartite chamber composed of three chambers of equal size (20×40 cm), two cylindrical cages, one empty and one containing an unfamiliar mouse, were placed in the lateral chambers. For 10 min, the mouse had access to all chambers. The preference for the unfamiliar mouse over the empty cage was assessed by calculating the ratio of time spent with the unfamiliar mouse over the time spent in the empty cage. The ratio of time spent in the chamber of the unfamiliar mouse over the time spent in the empty cage chamber was also calculated. The behavior of the animals was recorded using a camera. Measurements were performed with anymaze software.

Social proximity test

The social proximity test was performed as described elsewhere (Defensor et al., 2011). The test mouse was placed together with an unfamiliar mouse in a testing cage (7 cm×14 cm; transparent walls, custom made). For 10 min, social interaction was recorded using a video camera and viewer software (Biobserve). Nose tip-to-nose tip contact (NN), nose-to-head contact (NH) and nose-to-anogenital contact (NA) were counted over time.

Prepulse inhibition test

The prepulse inhibition (PPI) test, also known as startle reduction or reflex modification test, is a behavioral test in which a weak stimulus (prepulse) can reduce the startle response to an originally stronger startle stimulus (pulse). Reduced PPI is considered to be a biomarker of schizophrenia (Mena et al., 2016). The PPI of startle reflex was determined using a standard startle chamber (San Diego Instruments) according to the manufacturer's instructions as previously described (Mattei et al., 2014). The test started with 5 min habituation where the mouse was exposed to white noise of 65 decibels (dB). After the habituation session, a pseudorandomized session started with 10 different types of trials: eight acoustic startle pulse alone (120 dB) and 10 different prepulses followed by pulse trials were applied in which mice were exposed to either 69, 73 or 81 dB stimulus 100 ms before the pulse. In a random duration of 10-25 s, the trials were separated by 65 dB with noise. In the prepulse plus startle-pulse trials, the amount of PPI is measured and expressed as percentage of the basal startle response (startle pulse alone).

Statistics

Results are in general presented in box and whisker plots. For behavior analyses, results are expressed as mean±s.e.m. Samples were tested for normal distribution using the Shapiro-Wilk test and outliers using the GraphPad outlier calculator (https://www.graphpad.com/quickcalcs/Grubbs1.cfm). For statistical analysis, *t*-test was used (two-tailed), for nonparametric distribution Mann–Whitney *U*-test was performed. All

graphics and statistical analysis were performed using the Graph Pad Prism 5.0 software.

Acknowledgements
We thank Prof. Helmut Kettenmann (Cellular Neuroscience, Max-Delbrueck-Center for Molecular Medicine) for helpful discussion and revision of the manuscript. We thank Dr Li-Jin Chew (Center for Neuroscience Research, Children's Research Institute, Children's National Medical Center, Washington DC, USA) for manuscript editing. We thank Mrs Evelyn Strauss and Mrs Ruth Herrmann for help with paraffin wax sections and western blots.

Competing interests
The authors declare no competing or financial interests.

Author contributions
Conceptualization: T. Scheuer, S.A.W., I.V., T. Schmitz; Methodology: T. Scheuer, S.G., S.A.W., D.M., Y.S., P.C.B., S.E., I.V., T. Schmitz; Validation: T. Scheuer, I.V., T. Schmitz; Formal analysis: T. Scheuer, E.a.d.B., S.G., D.M., Y.S., P.C.B., V.F.; Investigation: T. Scheuer, E.a.d.B., S.G., T. Schmitz; Resources: T. Scheuer, S.A.W., S.E., C.B., I.V., T. Schmitz; Data curation: T. Scheuer, S.G.; Writing - original draft: T. Scheuer, T. Schmitz; Writing - review & editing: T. Scheuer, S.A.W., S.E., C.B., T. Schmitz; Visualization: T. Scheuer, E.a.d.B., S.G.; Supervision: T. Scheuer, T. Schmitz; Project administration: T. Scheuer; Funding acquisition: T. Scheuer, C.B., T. Schmitz.

Funding
This work was supported by Deutsche Forschungsgemeinschaft (SCHE 2078/2-1) (T. Scheuer), Förderverein für frühgeborene Kinder an der Charité (T. Schmitz and V.F.) and the Berlin Institute of Health (BIH) clinical scientist program (Y.S.).

References
Achim, K., Salminen, M. and Partanen, J. (2014). Mechanisms regulating GABAergic neuron development. *Cell. Mol. Life Sci. CMLS* **71**, 1395-1415. doi:10.1007/s00018-013-1501-3

Alcántara, S., de Lecea, L., Del Río, J. A., Ferrer, I. and Soriano, E. (1996). Transient colocalization of parvalbumin and calbindin D28k in the postnatal cerebral cortex: evidence for a phenotypic shift in developing nonpyramidal neurons. *Eur. J. Neurosci.* **8**, 1329-1339. doi:10.1111/j.1460-9568.1996.tb01595.x

Alifragis, P., Liapi, A. and Parnavelas, J. G. (2004). Lhx6 regulates the migration of cortical interneurons from the ventral telencephalon but does not specify their GABA phenotype. *J. Neurosci. Off. J. Soc. Neurosci.* **24**, 5643-5648. doi:10.1523/JNEUROSCI.1245-04.2004

American Psychiatric Association and American Psychiatric Association (eds.). (2013). *Diagnostic and Statistical Manual of Mental Disorders: DSM-5*, 5th edn. Washington, DC: American Psychiatric Association.

Arpi, E. and Ferrari, F. (2013). Preterm birth and behaviour problems in infants and preschool-age children: a review of the recent literature. *Dev. Med. Child Neurol.* **55**, 788-796. doi:10.1111/dmcn.12142

Arshad, A., Vose, L. R., Vinukonda, G., Hu, F., Yoshikawa, K., Csiszar, A., Brumberg, J. C. and Ballabh, P. (2016). Extended production of cortical interneurons into the third trimester of human gestation. *Cereb. Cortex* **26**, 2242-2256. doi:10.1093/cercor/bhv074

Benamer, N., Vidal, M. and Angulo, M. C. (2020). The cerebral cortex is a substrate of multiple interactions between GABAergic interneurons and oligodendrocyte lineage cells. *Neurosci. Lett.* **715**, 134615. doi:10.1016/j.neulet.2019.134615

Bendix, I., Schulze, C., von Haefen, C., Gellhaus, A., Endesfelder, S., Heumann, R., Felderhoff-Mueser, U. and Sifringer, M. (2012). Erythropoietin modulates autophagy signaling in the developing rat brain in an in vivo model of oxygen-toxicity. *Int. J. Mol. Sci.* **13**, 12939-12951. doi:10.3390/ijms131012939

Bicks, L. K., Yamamuro, K., Flanigan, M. E., Kim, J. M., Kato, D., Lucas, E. K., Koike, H., Peng, M. S., Brady, D. M., Chandrasekaran, S. et al. (2020). Prefrontal parvalbumin interneurons require juvenile social experience to establish adult social behavior. *Nat. Commun.* **11**, 1003. doi:10.1038/s41467-020-14740-z

Brill, C., Scheuer, T., Bührer, C., Endesfelder, S. and Schmitz, T. (2017). Oxygen impairs oligodendroglial development via oxidative stress and reduced expression of HIF-1α. *Sci. Rep.* **7**, 43000. doi:10.1038/srep43000

Cabungcal, J.-H., Steullet, P., Kraftsik, R., Cuenod, M. and Do, K. Q. (2013). Early-life insults impair parvalbumin interneurons via oxidative stress: reversal by N-acetylcysteine. *Biol. Psychiatry* **73**, 574-582. doi:10.1016/j.biopsych.2012.09.020

Canty, A. J., Dietze, J., Harvey, M., Enomoto, H., Milbrandt, J. and Ibáñez, C. F. (2009). Regionalized loss of parvalbumin interneurons in the cerebral cortex of mice with deficits in GFRalpha1 signaling. *J. Neurosci. Off. J. Soc. Neurosci.* **29**, 10695-10705. doi:10.1523/JNEUROSCI.2658-09.2009

Castillo, A., Sola, A., Baquero, H., Neira, F., Alvis, R., Deulofeut, R. and Critz, A. (2008). Pulse oxygen saturation levels and arterial oxygen tension values in newborns receiving oxygen therapy in the neonatal intensive care unit: is 85% to 93% an acceptable range? *Pediatrics* **121**, 882-889. doi:10.1542/peds.2007-0117

Collins, M. P., Lorenz, J. M., Jetton, J. R. and Paneth, N. (2001). Hypocapnia and other ventilation-related risk factors for cerebral palsy in low birth weight infants. *Pediatr. Res.* **50**, 712-719. doi:10.1203/00006450-200112000-00014

Dammann, O. and Leviton, A. (2004). Inflammatory brain damage in preterm newborns–dry numbers, wet lab, and causal inferences. *Early Hum. Dev.* **79**, 1-15. doi:10.1016/j.earlhumdev.2004.04.009

de Kieviet, J. F., Piek, J. P., Aarnoudse-Moens, C. S. and Oosterlaan, J. (2009). Motor development in very preterm and very low-birth-weight children from birth to adolescence: a meta-analysis. *JAMA* **302**, 2235-2242. doi:10.1001/jama.2009.1708

de Lecea, L., del Río, J. A. and Soriano, E. (1995). Developmental expression of parvalbumin mRNA in the cerebral cortex and hippocampus of the rat. *Brain Res. Mol. Brain Res.* **32**, 1-13. doi:10.1016/0169-328X(95)00056-X

De Leonibus, E., Managò, F., Giordani, F., Petrosino, F., Lopez, S., Oliverio, A., Amalric, M. and Mele, A. (2009). Metabotropic glutamate receptors 5 blockade reverses spatial memory deficits in a mouse model of Parkinson's disease. *Neuropsychopharmacol. Off. Publ. Am. Coll. Neuropsychopharmacol.* **34**, 729-738. doi:10.1038/npp.2008.129

Defensor, E. B., Pearson, B. L., Pobbe, R. L. H., Bolivar, V. J., Blanchard, D. C. and Blanchard, R. J. (2011). A novel social proximity test suggests patterns of social avoidance and gaze aversion-like behavior in BTBR T+ tf/J mice. *Behav. Brain Res.* **217**, 302-308. doi:10.1016/j.bbr.2010.10.033

Edden, R. A. E., Crocetti, D., Zhu, H., Gilbert, D. L. and Mostofsky, S. H. (2012). Reduced GABA concentration in attention-deficit/hyperactivity disorder. *Arch. Gen. Psychiatry* **69**, 750-753. doi:10.1001/archgenpsychiatry.2011.2280

Endesfelder, S., Zaak, I., Weichelt, U., Bührer, C. and Schmitz, T. (2014). Caffeine protects neuronal cells against injury caused by hyperoxia in the immature brain. *Free Radic. Biol. Med.* **67**, 221-234. doi:10.1016/j.freeradbiomed.2013.09.026

Endesfelder, S., Weichelt, U., Strauß, E., Schlör, A., Sifringer, M., Scheuer, T., Bührer, C. and Schmitz, T. (2017). Neuroprotection by Caffeine in hyperoxia-induced neonatal brain injury. *Int. J. Mol. Sci.* **18**, 187. doi:10.3390/ijms18010187

Felderhoff-Mueser, U., Bittigau, P., Sifringer, M., Jarosz, B., Korobowicz, E., Mahler, L., Piening, T., Moysich, A., Grune, T., Thor, F. et al. (2004). Oxygen causes cell death in the developing brain. *Neurobiol. Dis.* **17**, 273-282. doi:10.1016/j.nbd.2004.07.019

Feng, L., Zhao, T. and Kim, J. (2015). neuTube 1.0: a new design for efficient neuron reconstruction software based on the SWC format. *eNeuro* **2**, ENEURO.0049-14.2014. doi:10.1523/ENEURO.0049-14.2014

Ferguson, B. R. and Gao, W.-J. (2018). PV interneurons: critical regulators of e/i balance for prefrontal cortex-dependent behavior and psychiatric disorders. *Front. Neural Circuits* **12**, 37. doi:10.3389/fncir.2018.00037

Fields, R. D. (2008). White matter in learning, cognition and psychiatric disorders. *Trends Neurosci.* **31**, 361-370. doi:10.1016/j.tins.2008.04.001

Filice, F. and Schwaller, B. (2017). Parvalbumin and autism: different causes, same effect? *Oncotarget* **8**, 7222-7223. doi:10.18632/oncotarget.14238

Gao, R. and Penzes, P. (2015). Common mechanisms of excitatory and inhibitory imbalance in schizophrenia and autism spectrum disorders. *Curr. Mol. Med.* **15**, 146-167. doi:10.2174/1566524015666150303003028

Girgenti, M. J., Wohleb, E. S., Mehta, S., Ghosal, S., Fogaca, M. V. and Duman, R. S. (2019). Prefrontal cortex interneurons display dynamic sex-specific stress-induced transcriptomes. *Transl. Psychiatry* **9**, 292. doi:10.1038/s41398-019-0642-z

Guzman, S. J., Schlögl, A. and Schmidt-Hieber, C. (2014). Stimfit: quantifying electrophysiological data with Python. *Front. Neuroinformatics* **8**, 16. doi:10.3389/fninf.2014.00016

Habermacher, C., Angulo, M. C. and Benamer, N. (2019). Glutamate versus GABA in neuron-oligodendroglia communication. *Glia* **67**, 2092-2106. doi:10.1002/glia.23618

Hashemi, E., Ariza, J., Rogers, H., Noctor, S. C. and Martínez-Cerdeño, V. (2017). The number of parvalbumin-expressing interneurons is decreased in the prefrontal cortex in autism. *Cereb. Cortex* **27**, 1931-1943. doi:10.1093/cercor/bhw021

Haynes, R. L., Folkerth, R. D., Trachtenberg, F. L., Volpe, J. J. and Kinney, H. C. (2009). Nitrosative stress and inducible nitric oxide synthase expression in periventricular leukomalacia. *Acta Neuropathol. (Berl.)* **118**, 391-399. doi:10.1007/s00401-009-0540-1

Hines, M. L. and Carnevale, N. T. (1997). The NEURON simulation environment. *Neural Comput.* **9**, 1179-1209. doi:10.1162/neco.1997.9.6.1179

Hu, H., Gan, J. and Jonas, P. (2014). Interneurons. Fast-spiking, parvalbumin$^+$ GABAergic interneurons: from cellular design to microcircuit function. *Science* **345**, 1255263. doi:10.1126/science.1255263

Hu, J. S., Vogt, D., Sandberg, M. and Rubenstein, J. L. (2017). Cortical interneuron development: a tale of time and space. *Development* **144**, 3867-3878. doi:10.1242/dev.132852

Ikonomidou, C. and Kaindl, A. M. (2011). Neuronal death and oxidative stress in the developing brain. *Antioxid. Redox Signal.* **14**, 1535-1550. doi:10.1089/ars.2010.3581

Inan, M., Zhao, M., Manuszak, M., Karakaya, C., Rajadhyaksha, A. M., Pickel, V. M., Schwartz, T. H., Goldstein, P. A. and Manfredi, G. (2016). Energy deficit in parvalbumin neurons leads to circuit dysfunction, impaired sensory gating and social disability. *Neurobiol. Dis.* **93**, 35-46. doi:10.1016/j.nbd.2016.04.004

Jiang, X. and Nardelli, J. (2016). Cellular and molecular introduction to brain development. *Neurobiol. Dis.* **92**, 3-17. doi:10.1016/j.nbd.2015.07.007

Jiang, Z., Rompala, G. R., Zhang, S., Cowell, R. M. and Nakazawa, K. (2013). Social isolation exacerbates schizophrenia-like phenotypes via oxidative stress in cortical interneurons. *Biol. Psychiatry* **73**, 1024-1034. doi:10.1016/j.biopsych.2012.12.004

Johnson, S. and Marlow, N. (2011). Preterm birth and childhood psychiatric disorders. *Pediatr. Res.* **69**, 11R-18R. doi:10.1203/PDR.0b013e318212faa0

Johnson, S., Hollis, C., Kochhar, P., Hennessy, E., Wolke, D. and Marlow, N. (2010). Psychiatric disorders in extremely preterm children: longitudinal finding at age 11 years in the EPICure study. *J. Am. Acad. Child Adolesc. Psychiatry* **49**, 453-463.e1. doi:10.1097/00004583-201005000-00006

Jovanovic, J. N. and Thomson, A. M. (2011). Development of cortical GABAergic innervation. *Front. Cell. Neurosci.* **5**, 14. doi:10.3389/fncel.2011.00014

Kilb, W. (2012). Development of the GABAergic system from birth to adolescence. *Neurosci. Rev. J. Bringing Neurobiol. Neurol. Psychiatry* **18**, 613-630. doi:10.1177/1073858411422114

Lacaille, H., Vacher, C.-M., Bakalar, D., O'Reilly, J. J., Salzbank, J. and Penn, A. A. (2019). Impaired interneuron development in a novel model of neonatal brain injury. *eNeuro* **6**, ENEURO.0300-18.2019. doi:10.1523/ENEURO.0300-18.2019

Lake, E. M. R., Finn, E. S., Noble, S. M., Vanderwal, T., Shen, X., Rosenberg, M. D., Spann, M. N., Chun, M. M., Scheinost, D. and Constable, R. T. (2019). The functional brain organization of an individual allows prediction of measures of social abilities transdiagnostically in autism and attention-deficit/hyperactivity disorder. *Biol. Psychiatry* **86**, 315-326. doi:10.1016/j.biopsych.2019.02.019

Larroque, B., Ancel, P.-Y., Marret, S., Marchand, L., André, M., Arnaud, C., Pierrat, V., Rozé, J.-C., Messer, J., Thiriez, G. et al. (2008). Neurodevelopmental disabilities and special care of 5-year-old children born before 33 weeks of gestation (the EPIPAGE study): a longitudinal cohort study. *Lancet* **371**, 813-820. doi:10.1016/S0140-6736(08)60380-3

Leviton, A., Allred, E., Kuban, K. C. K., Dammann, O., O'Shea, T. M., Hirtz, D., Schreiber, M. D., Paneth, N. and **ELGAN Study Investigators**. (2010). Early blood gas abnormalities and the preterm brain. *Am. J. Epidemiol.* **172**, 907-916. doi:10.1093/aje/kwq222

Limperopoulos, C., Bassan, H., Sullivan, N. R., Soul, J. S., Robertson, R. L., Moore, M., Ringer, S. A., Volpe, J. J. and du Plessis, A. J. (2008). Positive screening for autism in ex-preterm infants: prevalence and risk factors. *Pediatrics* **121**, 758-765. doi:10.1542/peds.2007-2158

Lin, L.-C. and Sibille, E. (2013). Reduced brain somatostatin in mood disorders: a common pathophysiological substrate and drug target? *Front. Pharmacol.* **4**, 110. doi:10.3389/fphar.2013.00110

Lindström, K., Lindblad, F. and Hjern, A. (2011). Preterm birth and attention-deficit/hyperactivity disorder in schoolchildren. *Pediatrics* **127**, 858-865. doi:10.1542/peds.2010-1279

Livak, K. J. and Schmittgen, T. D. (2001). Analysis of relative gene expression data using real-time quantitative PCR and the $2^{-\Delta\Delta CT}$ Method. *Methods San Diego Calif* **25**, 402-408. doi:10.1006/meth.2001.1262

Lodge, D. J., Behrens, M. M. and Grace, A. A. (2009). A loss of parvalbumin-containing interneurons is associated with diminished oscillatory activity in an animal model of schizophrenia. *J. Neurosci. Off. J. Soc. Neurosci.* **29**, 2344-2354. doi:10.1523/JNEUROSCI.5419-08.2009

Lussier, S. J. and Stevens, H. E. (2016). Delays in GABAergic interneuron development and behavioral inhibition after prenatal stress. *Dev. Neurobiol.* **76**, 1078-1091. doi:10.1002/dneu.22376

Manent, J.-B. and Represa, A. (2007). Neurotransmitters and brain maturation: early paracrine actions of GABA and glutamate modulate neuronal migration. *Neurosci. Rev. J. Bringing Neurobiol. Neurol. Psychiatry* **13**, 268-279. doi:10.1177/1073858406298918

Mattei, D., Djodari-Irani, A., Hadar, R., Pelz, A., de Cossío, L. F., Goetz, T., Matyash, M., Kettenmann, H., Winter, C. and Wolf, S. A. (2014). Minocycline rescues decrease in neurogenesis, increase in microglia cytokines and deficits in sensorimotor gating in an animal model of schizophrenia. *Brain. Behav. Immun.* **38**, 175-184. doi:10.1016/j.bbi.2014.01.019

Mattei, D., Ivanov, A., Ferrai, C., Jordan, P., Guneykaya, D., Buonfiglioli, A., Schaafsma, W., Przanowski, P., Deuther-Conrad, W., Brust, P. et al. (2017). Maternal immune activation results in complex microglial transcriptome signature in the adult offspring that is reversed by minocycline treatment. *Transl. Psychiatry* **7**, e1120. doi:10.1038/tp.2017.80

Mena, A., Ruiz-Salas, J. C., Puentes, A., Dorado, I., Ruiz-Veguilla, M. and De la Casa, L. G. (2016). Reduced prepulse inhibition as a biomarker of Schizophrenia. *Front. Behav. Neurosci.* **10**, 202. doi:10.3389/fnbeh.2016.00202

Miyamae, T., Chen, K., Lewis, D. A. and Gonzalez-Burgos, G. (2017). Distinct physiological maturation of parvalbumin-positive neuron subtypes in mouse prefrontal cortex. *J. Neurosci. Off. J. Soc. Neurosci.* **37**, 4883-4902. doi:10.1523/JNEUROSCI.3325-16.2017

Nakazawa, K., Zsiros, V., Jiang, Z., Nakao, K., Kolata, S., Zhang, S. and Belforte, J. E. (2012). GABAergic interneuron origin of schizophrenia pathophysiology. *Neuropharmacology* **62**, 1574-1583. doi:10.1016/j.neuropharm.2011.01.022

Northoff, G. and Sibille, E. (2014). Why are cortical GABA neurons relevant to internal focus in depression? A cross-level model linking cellular, biochemical and neural network findings. *Mol. Psychiatry* **19**, 966-977. doi:10.1038/mp.2014.68

Orduz, D., Maldonado, P. P., Balia, M., Vélez-Fort, M., de Sars, V., Yanagawa, Y., Emiliani, V. and Angulo, M. C. (2015). Interneurons and oligodendrocyte progenitors form a structured synaptic network in the developing neocortex. *eLife* **4**, e06953. doi:10.7554/eLife.06953

Panda, S., Dohare, P., Jain, S., Parikh, N., Singla, P., Mehdizadeh, R., Klebe, D. W., Kleinman, G. M., Cheng, B. and Ballabh, P. (2018). Estrogen treatment reverses prematurity-induced disruption in cortical interneuron population. *J. Neurosci. Off. J. Soc. Neurosci.* **38**, 7378-7391. doi:10.1523/JNEUROSCI.0478-18.2018

Panthi, S. and Leitch, B. (2019). The impact of silencing feed-forward parvalbumin-expressing inhibitory interneurons in the cortico-thalamocortical network on seizure generation and behaviour. *Neurobiol. Dis.* **132**, 104610. doi:10.1016/j.nbd.2019.104610

Penn, A. A., Gressens, P., Fleiss, B., Back, S. A. and Gallo, V. (2016). Controversies in preterm brain injury. *Neurobiol. Dis.* **92**, 90-101. doi:10.1016/j.nbd.2015.10.012

Powell, S. B., Sejnowski, T. J. and Behrens, M. M. (2012). Behavioral and neurochemical consequences of cortical oxidative stress on parvalbumin-interneuron maturation in rodent models of schizophrenia. *Neuropharmacology* **62**, 1322-1331. doi:10.1016/j.neuropharm.2011.01.049

Pöyhönen, S., Er, S., Domanskyi, A. and Airavaara, M. (2019). Effects of neurotrophic factors in glial cells in the central nervous system: expression and properties in neurodegeneration and injury. *Front. Physiol.* **10**, 486. doi:10.3389/fphys.2019.00486

Pozas, E. and Ibáñez, C. F. (2005). GDNF and GFRα1 promote differentiation and tangential migration of cortical GABAergic neurons. *Neuron* **45**, 701-713. doi:10.1016/j.neuron.2005.01.043

Raabe, F. J., Slapakova, L., Rossner, M. J., Cantuti-Castelvetri, L., Simons, M., Falkai, P. G. and Schmitt, A. (2019). Oligodendrocytes as a new therapeutic target in schizophrenia: from histopathological findings to neuron-oligodendrocyte interaction. *Cells* **8**, 1496. doi:10.3390/cells8121496

Richter-Landsberg, C. and Heinrich, M. (1996). OLN-93: a new permanent oligodendroglia cell line derived from primary rat brain glial cultures. *J. Neurosci. Res.* **45**, 161-173. doi:10.1002/(SICI)1097-4547(19960715)45:2<161::AID-JNR8>3.0.CO;2-8

Ritter, J., Schmitz, T., Chew, L.-J., Bührer, C., Möbius, W., Zonouzi, M. and Gallo, V. (2013). Neonatal hyperoxia exposure disrupts axon-oligodendrocyte integrity in the subcortical white matter. *J. Neurosci. Off. J. Soc. Neurosci.* **33**, 8990-9002. doi:10.1523/JNEUROSCI.5528-12.2013

Rodgers, R. J. and Dalvi, A. (1997). Anxiety, defence and the elevated plus-maze. *Neurosci. Biobehav. Rev.* **21**, 801-810. doi:10.1016/S0149-7634(96)00058-9

Rodrigues, C. A. V., Diogo, M. M., da Silva, C. L. and Cabral, J. M. S. (2010). Hypoxia enhances proliferation of mouse embryonic stem cell-derived neural stem cells. *Biotechnol. Bioeng.* **106**, 260-270. doi:10.1002/bit.22648

Rudy, B., Fishell, G., Lee, S. H. and Hjerling-Leffler, J. (2011). Three groups of interneurons account for nearly 100% of neocortical GABAergic neurons. *Dev. Neurobiol.* **71**, 45-61. doi:10.1002/dneu.20853

Sakurai, T. and Gamo, N. J. (2019). Cognitive functions associated with developing prefrontal cortex during adolescence and developmental neuropsychiatric disorders. *Neurobiol. Dis.* **131**, 104322. doi:10.1016/j.nbd.2018.11.007

Scheuer, T., Sharkovska, Y., Tarabykin, V., Marggraf, K., Brockmöller, V., Bührer, C., Endesfelder, S. and Schmitz, T. (2018). Neonatal hyperoxia perturbs neuronal development in the cerebellum. *Mol. Neurobiol.* **55**, 3901-3915. doi:10.1007/s12035-017-0612-5

Schmitz, T., Ritter, J., Mueller, S., Felderhoff-Mueser, U., Chew, L.-J. and Gallo, V. (2011). Cellular changes underlying hyperoxia-induced delay of white matter development. *J. Neurosci. Off. J. Soc. Neurosci.* **31**, 4327-4344. doi:10.1523/JNEUROSCI.3942-10.2011

Schmitz, T., Endesfelder, S., Reinert, M.-C., Klinker, F., Müller, S., Bührer, C. and Liebetanz, D. (2012). Adolescent hyperactivity and impaired coordination after neonatal hyperoxia. *Exp. Neurol.* **235**, 374-379. doi:10.1016/j.expneurol.2012.03.002

Schmitz, T., Krabbe, G., Weikert, G., Scheuer, T., Matheus, F., Wang, Y., Mueller, S., Kettenmann, H., Matyash, V., Bührer, C. et al. (2014). Minocycline protects the immature white matter against hyperoxia. *Exp. Neurol.* **254**, 153-165. doi:10.1016/j.expneurol.2014.01.017

Seibenhener, M. L. and Wooten, M. C. (2015). Use of the Open Field Maze to measure locomotor and anxiety-like behavior in mice. *J. Vis. Exp.* e52434. doi:10.3791/52434

Serdar, M., Herz, J., Kempe, K., Lumpe, K., Reinboth, B. S., Sizonenko, S. V., Hou, X., Herrmann, R., Hadamitzky, M., Heumann, R. et al. (2016). Fingolimod protects against neonatal white matter damage and long-term cognitive deficits caused by hyperoxia. *Brain. Behav. Immun.* **52**, 106-119. doi:10.1016/j.bbi.2015.10.004

Sorce, S., Krause, K.-H. and Jaquet, V. (2012). Targeting NOX enzymes in the central nervous system: therapeutic opportunities. *Cell. Mol. Life Sci.* **69**, 2387-2407. doi:10.1007/s00018-012-1014-5

Stolp, H. B., Fleiss, B., Arai, Y., Supramaniam, V., Vontell, R., Birtles, S., Yates, A. G., Baburamani, A. A., Thornton, C., Rutherford, M. et al. (2019). Interneuron development is disrupted in preterm brains with diffuse white matter injury: observations in mouse and human. *Front. Physiol.* **10**, 955. doi:10.3389/fphys.2019.00955

Strang, J. F., Kenworthy, L., Daniolos, P., Case, L., Wills, M. C., Martin, A. and Wallace, G. L. (2012). Depression and anxiety symptoms in children and adolescents with autism spectrum disorders without intellectual disability. *Res. Autism Spectr. Disord.* **6**, 406-412. doi:10.1016/j.rasd.2011.06.015

Tripodi, M., Bhandari, K., Chowdhury, A., Mukherjee, A. and Caroni, P. (2018). Parvalbumin interneuron plasticity for consolidation of reinforced learning. *Cold Spring Harb. Symp. Quant. Biol.* **83**, 25-35. doi:10.1101/sqb.2018.83.037630

Vasistha, N. A., Pardo-Navarro, M., Gasthaus, J., Weijers, D., Müller, M. K., García-González, D., Malwade, S., Korshunova, I., Pfisterer, U., von Engelhardt, J. et al. (2019). Maternal inflammation has a profound effect on cortical interneuron development in a stage and subtype-specific manner. *Mol. Psychiatry* **25**, 2313-2329. doi:10.1038/s41380-019-0539-5

Vasung, L., Abaci Turk, E., Ferradal, S. L., Sutin, J., Stout, J. N., Ahtam, B., Lin, P.-Y. and Grant, P. E. (2019). Exploring early human brain development with structural and physiological neuroimaging. *Neuroimage* **187**, 226-254. doi:10.1016/j.neuroimage.2018.07.041

Volpe, J. J. (2009). Brain injury in premature infants: a complex amalgam of destructive and developmental disturbances. *Lancet Neurol.* **8**, 110-124. doi:10.1016/S1474-4422(08)70294-1

Wang, G.-X., Ma, Y.-H., Wang, S.-F., Ren, G.-F. and Guo, H. (2012). Association of dopaminergic/GABAergic genes with attention deficit hyperactivity disorder in children. *Mol. Med. Rep.* **6**, 1093-1098. doi:10.3892/mmr.2012.1028

White, S. W., Oswald, D., Ollendick, T. and Scahill, L. (2009). Anxiety in children and adolescents with autism spectrum disorders. *Clin. Psychol. Rev.* **29**, 216-229. doi:10.1016/j.cpr.2009.01.003

Wilkins, A., Majed, H., Layfield, R., Compston, A. and Chandran, S. (2003). Oligodendrocytes promote neuronal survival and axonal length by distinct intracellular mechanisms: a novel role for oligodendrocyte-derived glial cell line-derived neurotrophic factor. *J. Neurosci.* **23**, 4967-4974. doi:10.1523/JNEUROSCI.23-12-04967.2003

Wöhr, M., Orduz, D., Gregory, P., Moreno, H., Khan, U., Vörckel, K. J., Wolfer, D. P., Welzl, H., Gall, D., Schiffmann, S. N. et al. (2015). Lack of parvalbumin in mice leads to behavioral deficits relevant to all human autism core symptoms and related neural morphofunctional abnormalities. *Transl. Psychiatry* **5**, e525. doi:10.1038/tp.2015.19

Wonders, C. P. and Anderson, S. A. (2006). The origin and specification of cortical interneurons. *Nat. Rev. Neurosci.* **7**, 687-696. doi:10.1038/nrn1954

Wyrsch, P., Blenn, C., Bader, J. and Althaus, F. R. (2012). Cell death and autophagy under oxidative stress: roles of poly(ADP-Ribose) polymerases and Ca(2+). *Mol. Cell. Biol.* **32**, 3541-3553. doi:10.1128/MCB.00437-12

Xia, F., Richards, B. A., Tran, M. M., Josselyn, S. A., Takehara-Nishiuchi, K. and Frankland, P. W. (2017). Parvalbumin-positive interneurons mediate neocortical-hippocampal interactions that are necessary for memory consolidation. *eLife* **6**, e27868. doi:10.7554/eLife.27868

Yang, P., Cai, G., Cai, Y., Fei, J. and Liu, G. (2013). Gamma aminobutyric acid transporter subtype 1 gene knockout mice: a new model for attention deficit/hyperactivity disorder. *Acta Biochim. Biophys. Sin.* **45**, 578-585. doi:10.1093/abbs/gmt043

Yoshida, Y., Umeno, A. and Shichiri, M. (2013). Lipid peroxidation biomarkers for evaluating oxidative stress and assessing antioxidant capacity in vivo. *J. Clin. Biochem. Nutr.* **52**, 9-16. doi:10.3164/jcbn.12-112

Zhang, K., Zhu, L. and Fan, M. (2011). Oxygen, a key factor regulating cell behavior during neurogenesis and cerebral diseases. *Front. Mol. Neurosci.* **4**, 5. doi:10.3389/fnmol.2011.00005

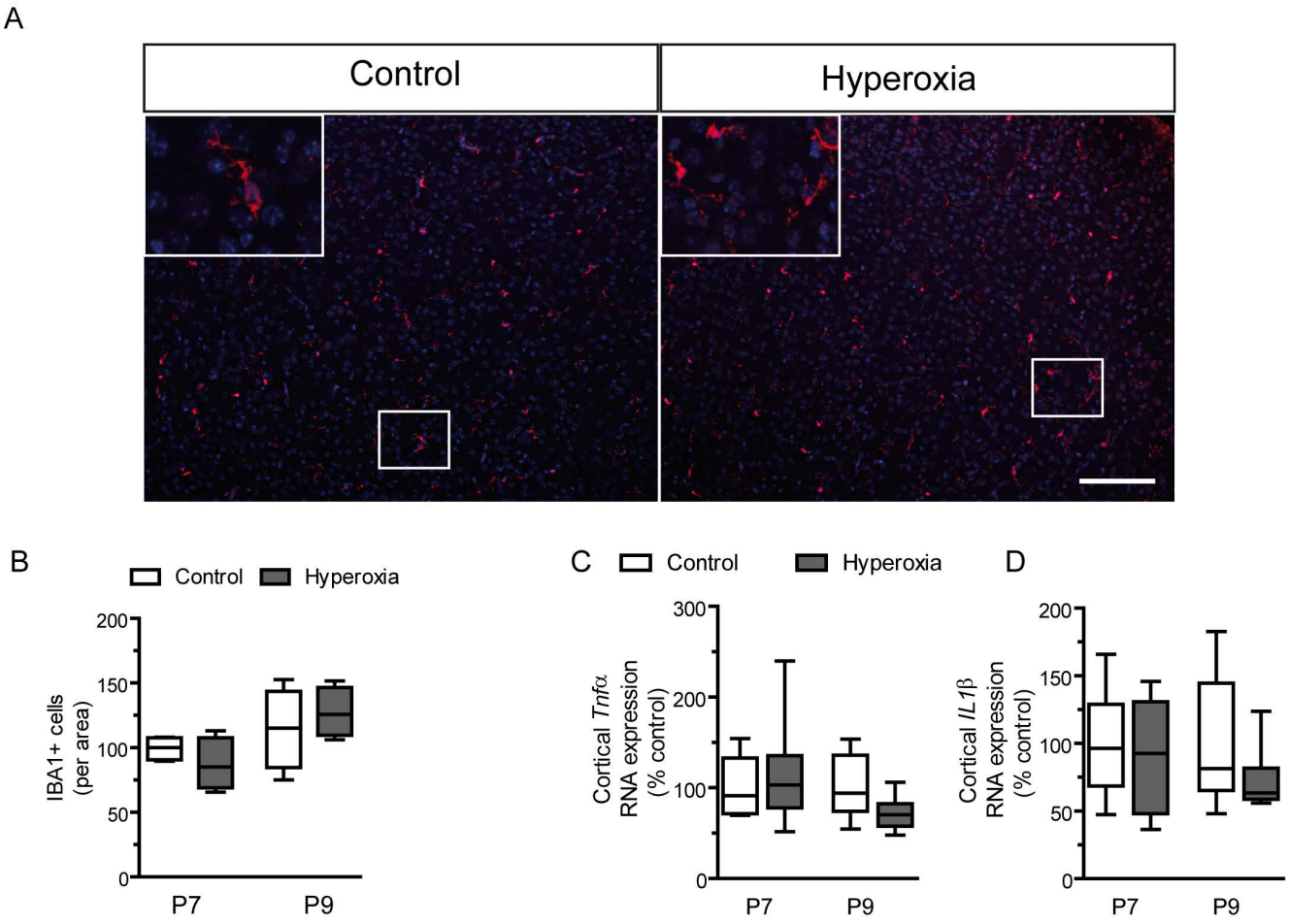

Fig. S1. Microglia response to hyperoxia exposure

IBA1 staining of 10 µm coronal brain section at the ages P7 and P9 (A). The number and the morphology of cortical IBA1+ microglia was not affected by neonatal oxygen exposure from P5 to P7 (B) (n = 4). RNA expression of cortical *Tnfα* (C) and *Il1β* (D) was similar in both groups (for qPCR: n = 8 (P7), 7 (P9))

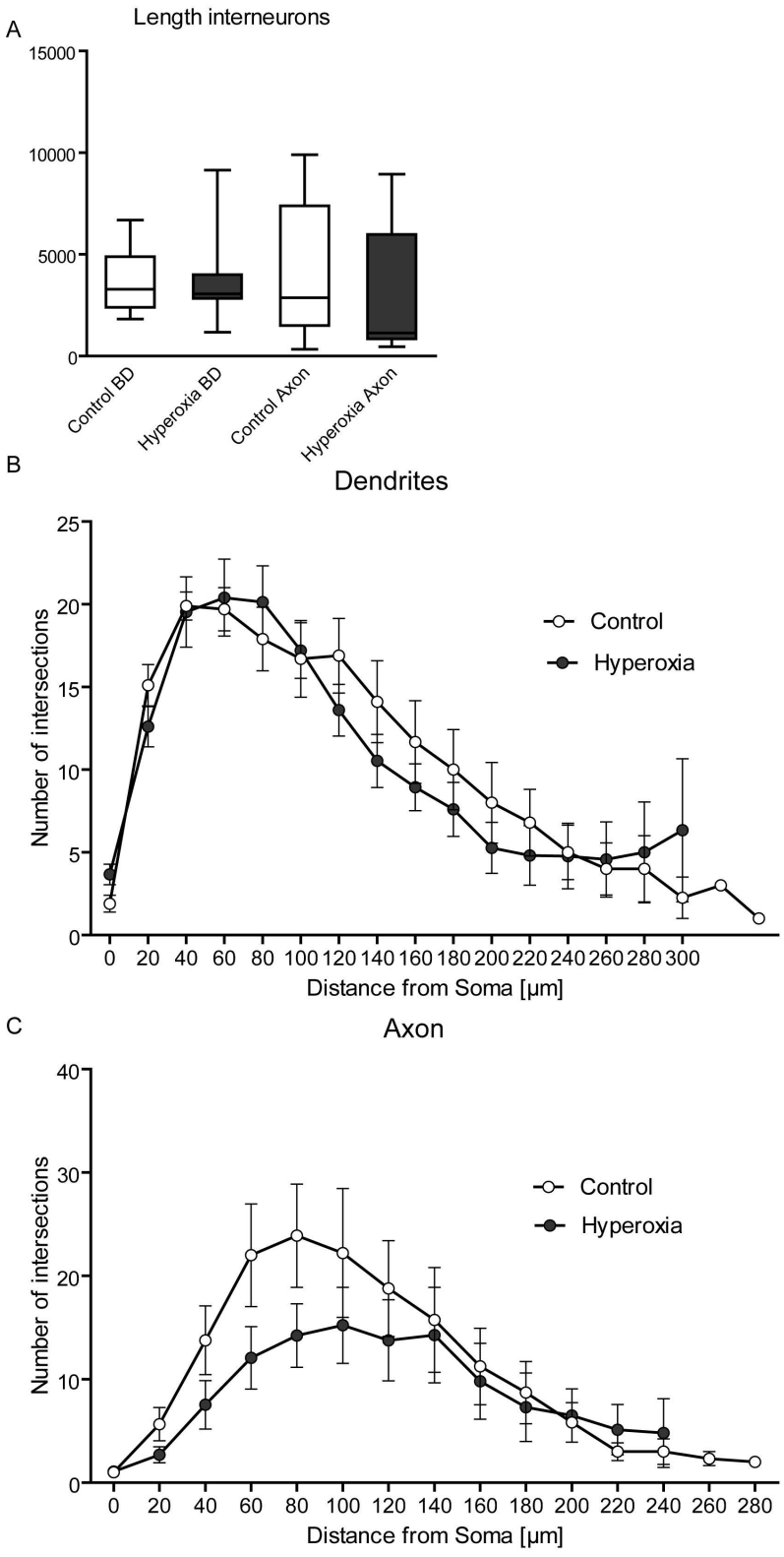

Fig. S2. Morphology of cortical Interneurons

Morphological analysis did not reveal any significant difference in dendritic length (A). Sholl analysis of basal dendrites (B) and axons (C) did not show changes in intersections (control n = 7 (12 PVALB+ interneurons), hyperoxia n = 12 (15 PVALB+ interneurons)).

Table S1. Oligonucleotides

Gene		Forward Primer	Reverse Primer	Probe	Detection
Atg3	NM_026402.3	TAGTGGAAGCCT GCAAAGCTA	GTGGGAGATGAG GATGGTTTT		SYBR Green
Atg12	NM_026217.3	GCTGAAGGCTGT AGGAGACACT	ACCATCACTGCC AAAACACTC		SYBR Green
Casp3	NM_001284409.1	ATGGGAGCAAGT CAGTGGAC	ATTTCAGGCCCA TGAATGTC	TGTCATCTCGC TCTGGTACG	TaqMan
Cnp	NM_001146318.1	AGCAGGAGGTGG TGAAGAGA	GATGGCTTGTCC AGATCA	TTTGTGACACC CAAGACAGC	TaqMan
Gclc	NM_010295.2	GTGGAGGCCAAT ATGAGGAA	CTGGGTTGGGTC TGTGTTCT	AGGCTCTCTGC ACCATCACT	TaqMan
Gdnf	NM_001301332.1	TTTGAAGACGCC AGGGAAATG	TGTCCAGAATCA ACCACCAAG		SYBR Green
Hprt	NM_013556.2	TGCTCGAGATGT CATGAAGG	TATGTCCCCCGT TGACTGAT	ATCACATTGTG GCCCTCTGT	TaqMan
Il1β	NM_008361.4	TGACGGACCCCA AAAGATGA	TGCTGCTGCGAG ATTTGAAG	TGCTTCCAAAC CTTTGACCT	TaqMan
Lhx6	NM_008500.2	AAGGTAGAGCCT CCCCATGT	AGGTTGTTGACC TTGAGCAGA		SYBR Green
Olig2	NM_016967.2	ATCTTCCTCCAG CACCTCCT	GGGCTCAGTCAT CTGCTTCT	CCACGTCTTCC ACCAAGAAA	TaqMan
Pvalb	NM_001330686.1	GGCGATAGGAGC CTTTGCT	ACCTCATCCGGG TTCTTTTTC		SYBR Green
Reln	NM_011261.2	AGTGTGGCACCA TCATGCAT	TGTTGTTGTGTTC AGGCATGTG		SYBR Green
Sod2	NM_013671.3	CCGAGGAGAAGT ACCACGAG	ATATGTCCCCCA CCATTGAA	ACAACTCAGGT CGCTCTTCAG	TaqMan
Sst	NM_009215.1	CCCAGACTCCGT CAGTTTCTG	GGGCATCATTCT CTGTCTGGTT		SYBR Green
Tnfα	NM_013693.3	ACCACGCTCTTC TGTCTACTGAACT	TCTGGGCCATAG AACTGATGAGA	AAGGGATGAGA AGTTCCCAA	TaqMan
Vip	NM_011702.3	CTCTTCAGTGTG CTGTTCTCTCAGT	AAACGGCATCCT GTCATCCA		SYBR Green